

# Lattice QCD @ nonzero temperature and finite density

Heng-Tong Ding (丁亨通)

Central China Normal University, Wuhan

XXVIII International Symposium on Lepton Photon Interactions at High Energies

Aug. 7 - Aug. 12, 2017, in Guangzhou

# Symmetries of QCD in the vacuum

$$\mathcal{L} = -\frac{1}{4}F^{\mu\nu}F_{\mu\nu} + \sum_{q=u,d,s,c,b,t} \bar{q} \left[ i\gamma^\mu (\partial_\mu - igA_\mu) - m_q \right] q$$

**Classical QCD symmetry ( $m_q=0$ )**

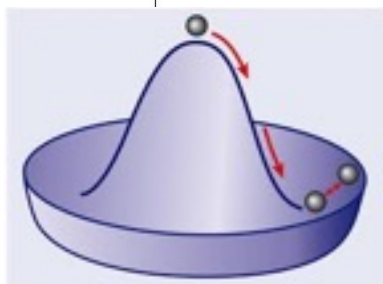
$$SU(N_f)_L \times SU(N_f)_R \times U(1)_V \times U(1)_A$$



**Quantum QCD vacuum ( $m_q=0$ )**

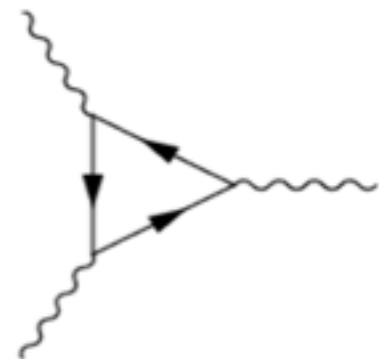
Chiral condensate:  
spontaneous mass generation

$$\langle \bar{q}_R q_L \rangle \neq 0$$



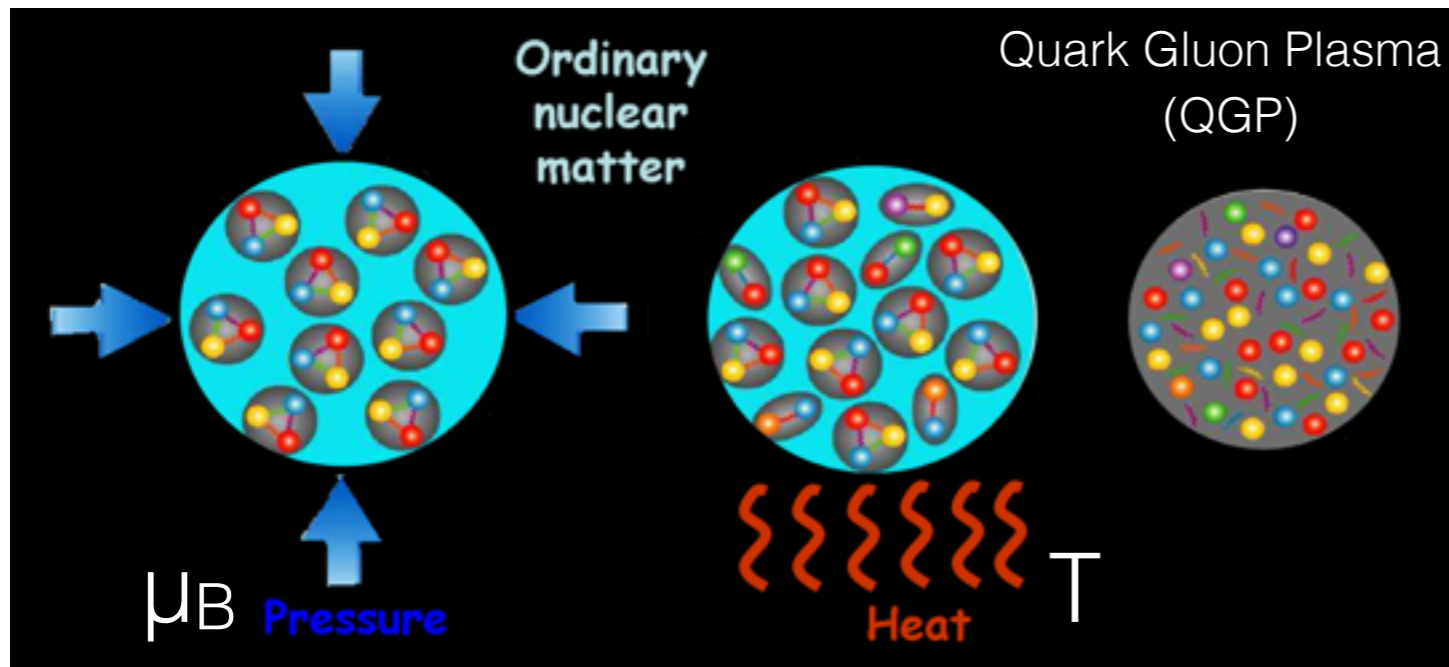
Axial anomaly:  
quantum violation of  $U(1)_A$

$$\partial_\mu j_5^\mu = \frac{g^2 N_f}{16\pi^2} \text{tr}(\tilde{F}_{\mu\nu} F^{\mu\nu})$$

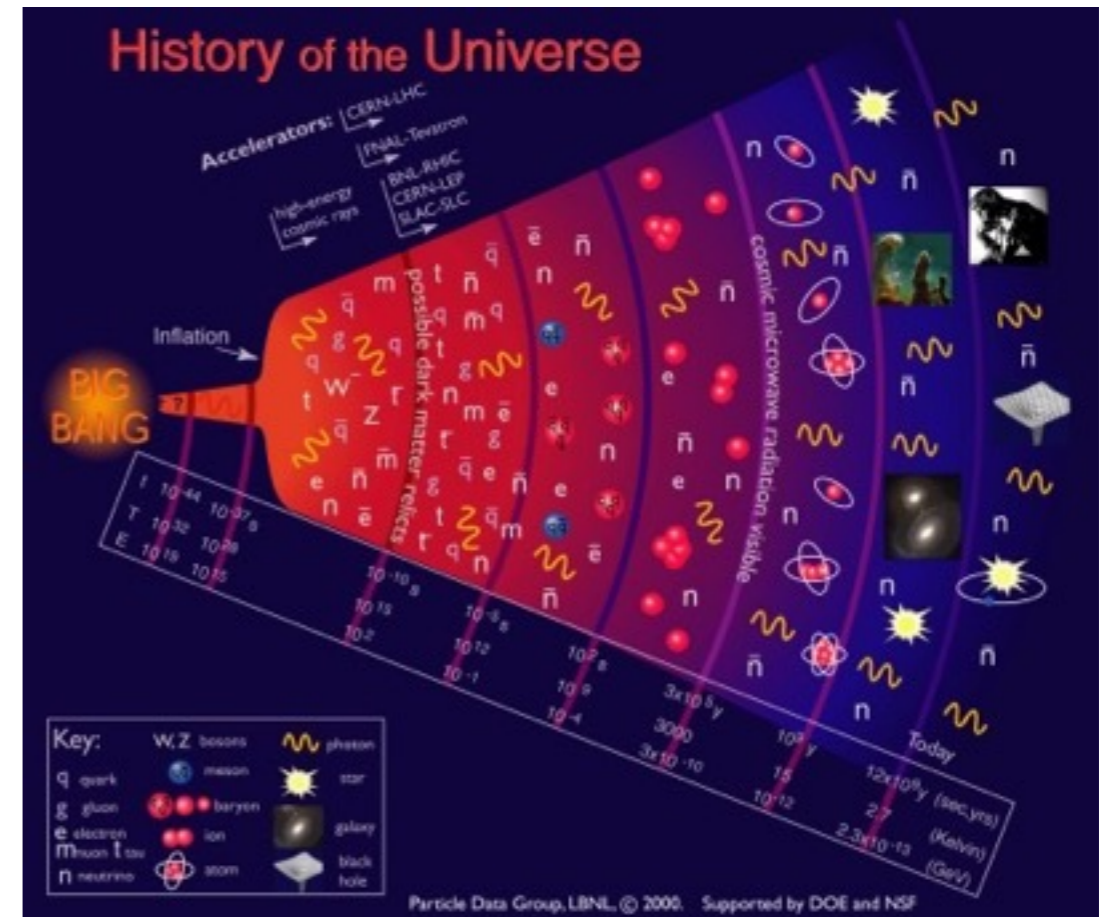


$$SU(N_f)_V \times U(1)_V$$

# Symmetry restoration in extreme conditions: QCD phase transitions



“The whole is more than sum of its parts.”  
Aristotle, *Metaphysica* 10f-1045a

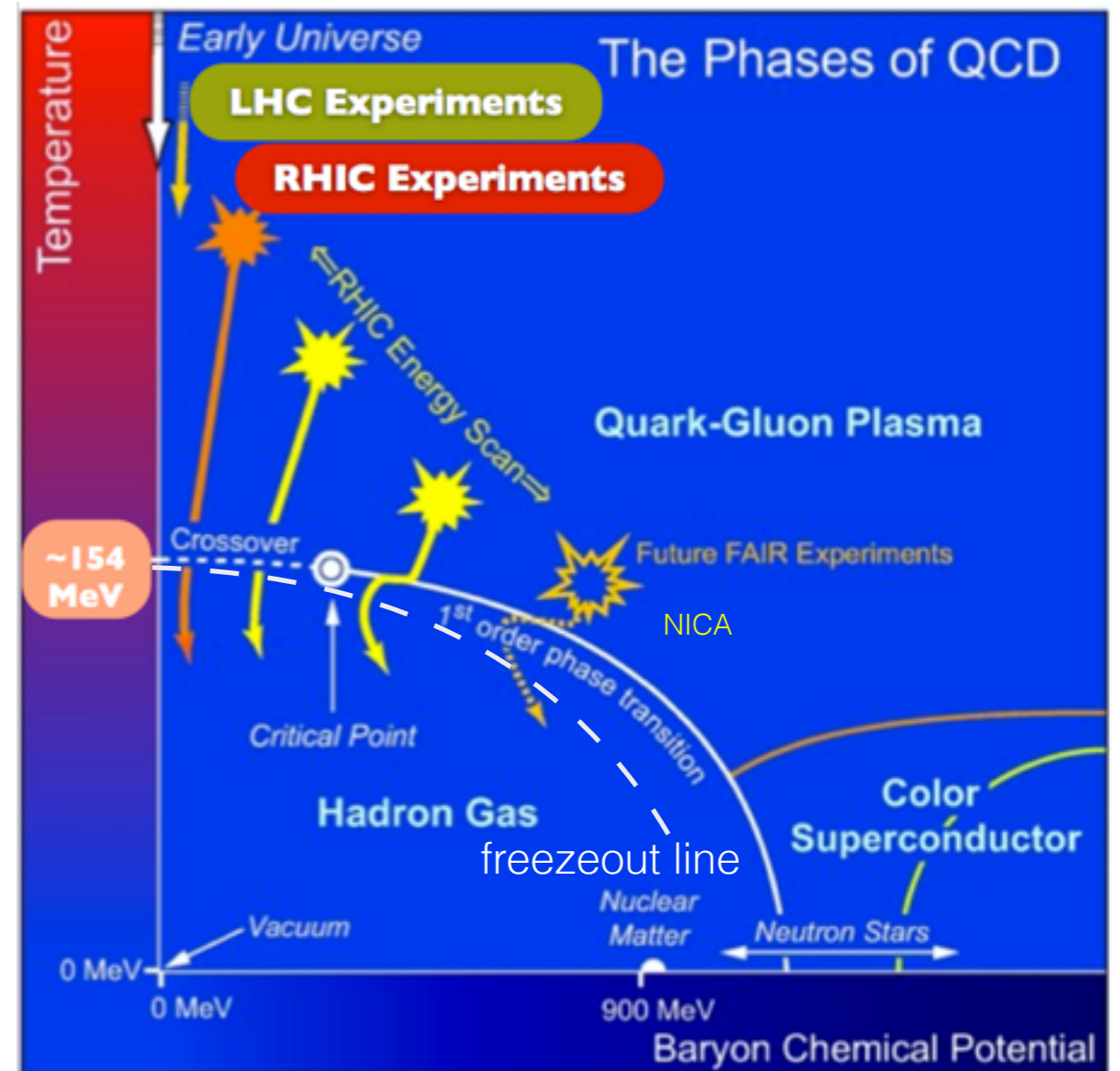
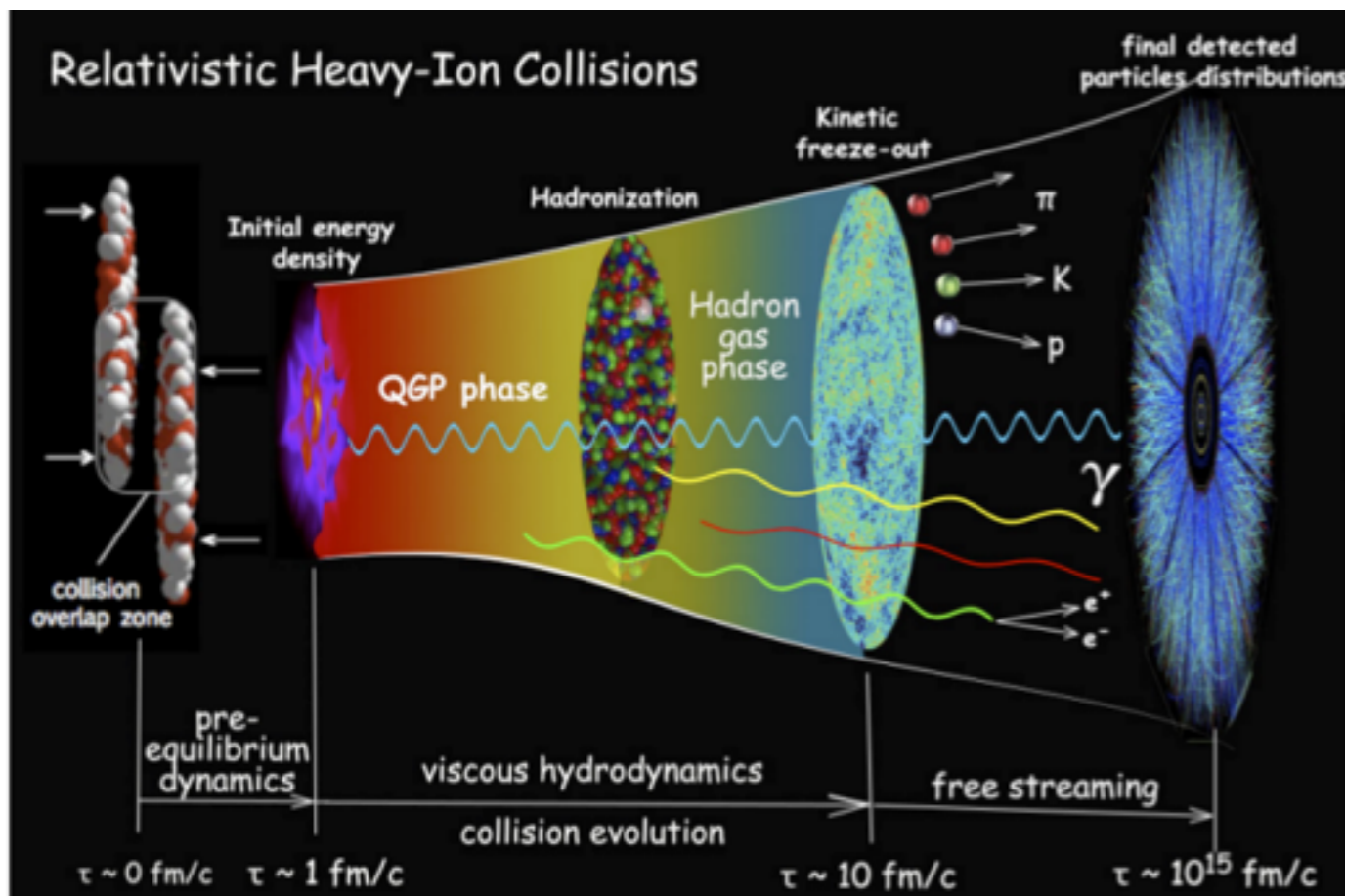


What are the phases of strong-interaction matter and what roles do they play in cosmos?

What are the  $T_c$ , orders and universality classes of (chiral & deconfinement) phase transitions?

What does QCD predict for the properties of the strong-interaction matter in extreme conditions?

# recreate QGP in Heavy Ion collisions...



QCD Equation of State for  $\sqrt{s_{NN}} \gtrsim 7.7$  GeV or  $\mu_B/T \lesssim 3$   
 possible location of Critical Point or window of criticality  
 proximity of the transition and freeze out lines

# Current hot & dense lattice QCD simulations

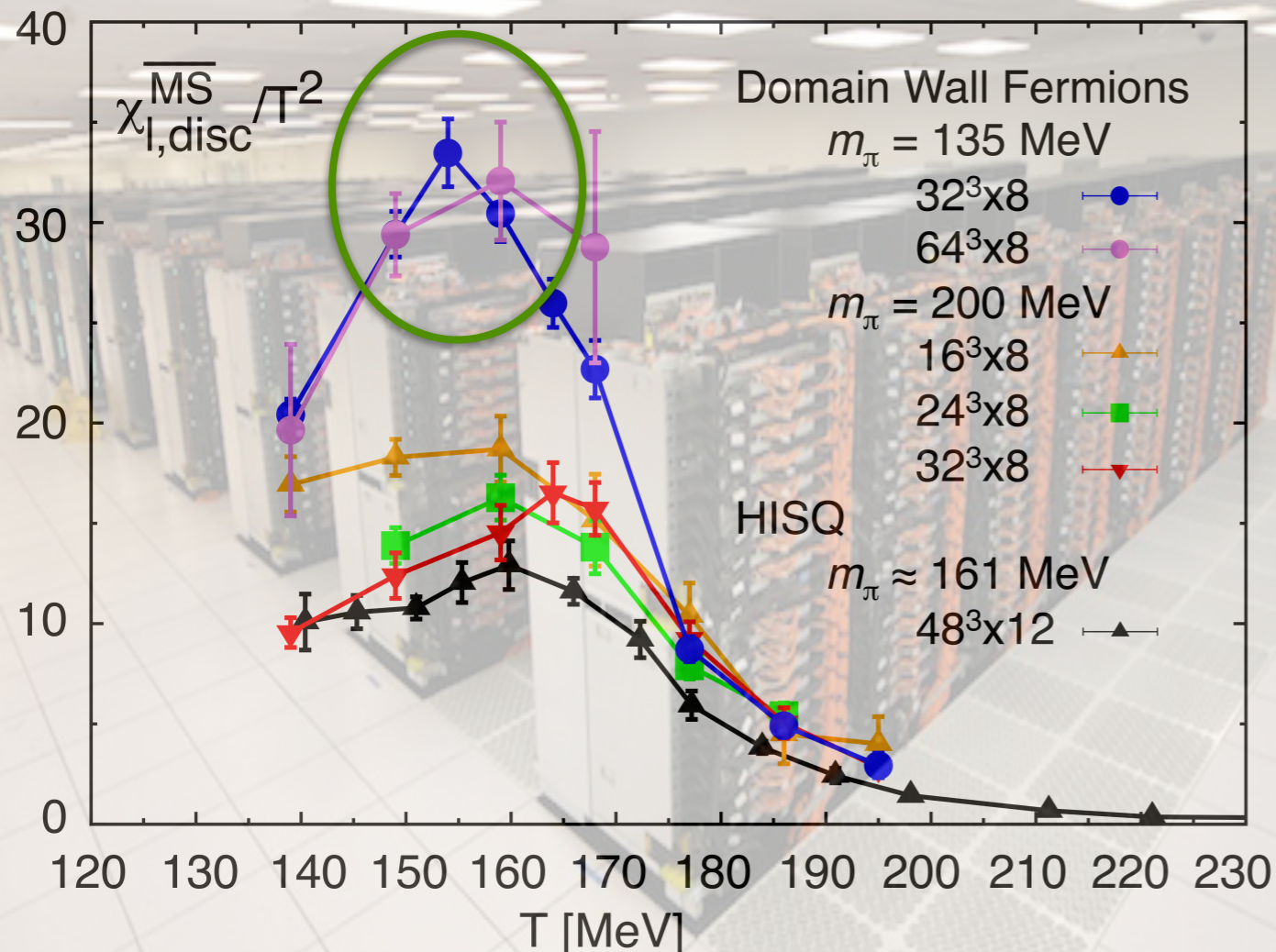
Lattice QCD: discretized version of QCD on a Euclidean space-time lattice, reproduces QCD when lattice spacing  $a \rightarrow 0$  (continuum limit)

Mostly dynamical QCD with  $N_f=2+1$  and physical pion mass

- ❖ Staggered actions at  $a \neq 0$ : taste symmetry breaking
  - ❖ 1 physical Goldstone pion +15 heavier unphysical pions
  - ❖ averaged pion mass, i.e. Root Mean Squared (RMS) pion mass
  - ❖ Smaller RMS pion mass  $\rightarrow$  Better improved action: HISQ, stout
- ❖ Chiral fermions(Domain Wall/Overlap) at  $a \neq 0$ 
  - ❖ preserves full flavor symmetry and chiral symmetries
  - ❖ computationally expensive to simulate, currently starts to produce interesting results on QCD thermodynamics

# Where do we stand now

transition from hadronic phase to QGP phase at  $\mu_B = 0$



HotQCD: PRL 113 (2014) 082001

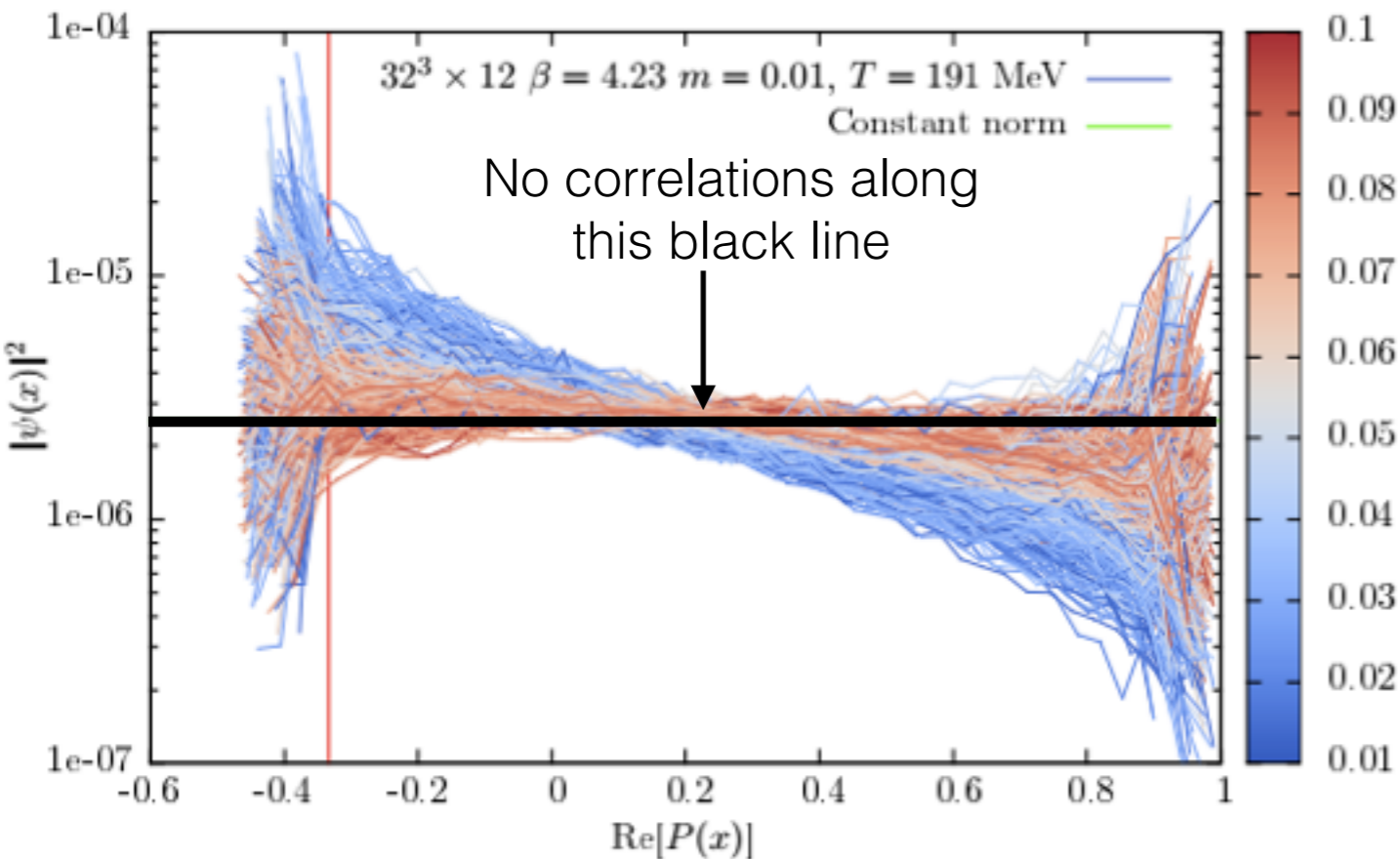
- Consistent results with 3 discretization schemes with  $m_\pi = 135$  MeV:  
Domain wall, HISQ, stout

$$T_{pc} = 155(1)(8) \text{ MeV}$$

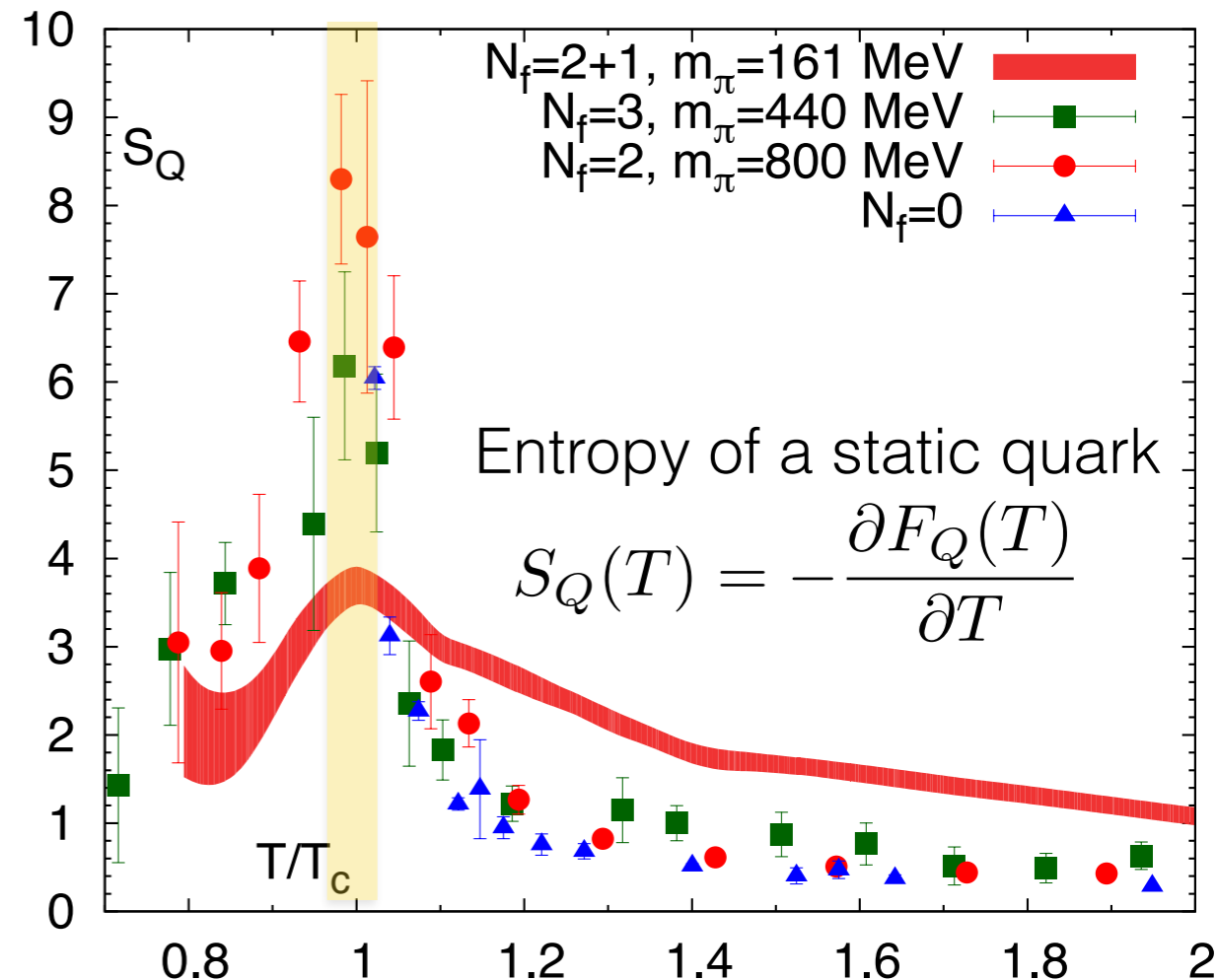
- Not a true (chiral or deconfinement) phase transition but a rapid chiral crossover

See also the consistent continuum extrapolated results of HISQ, stout, and overlap in:  
Wuppertal-Budapest: Nature 443(2006)675, JHEP 1009 (2010) 073 , HotQCD: PRD 85 (2012)054503  
Borsanyi et al., [WB collaboration], arXiv: 1510.03376, Phys.Lett. B713 (2012) 342

# Possible connections between chiral and deconfinement aspects of the transition



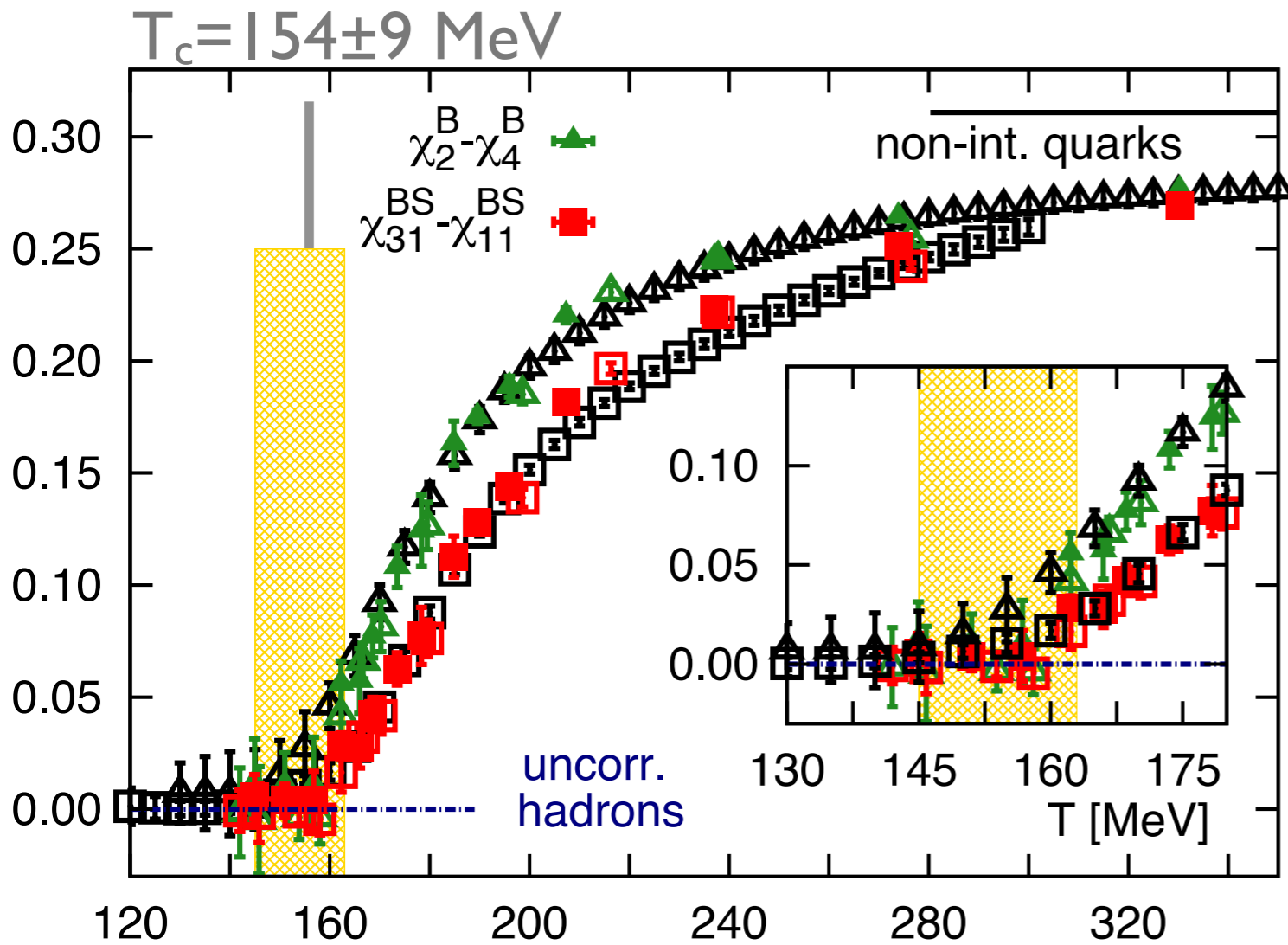
G. Cossu and S. Hashimoto, JHEP 1606 (2016) 056



A. Bazavov, N. Brambilla, HTD et al., PRD93 (2016) no.11, 114502

- 📍 Near zero eigenmodes are correlated with Polyakov loop
- 📍 Overlap of the peak locations of  $S_Q$  in QCD with different  $N_f$

# Deconfinement of hadrons carrying strangeness



HTD, F. Karsch, S. Mukherjee, arXiv:1504.05274

fluctuations of baryon numbers and strangeness

$$\chi_{mn}^{BS} = \left. \frac{\partial^{m+n} (p(\hat{\mu}_B, \hat{\mu}_S)/T^4)}{\partial \hat{\mu}_B^m \partial \hat{\mu}_S^n} \right|_{\hat{\mu}=0}$$

$\chi_{2^B}^B - \chi_{4^B}^B$ : receives contributions from all **hadrons**

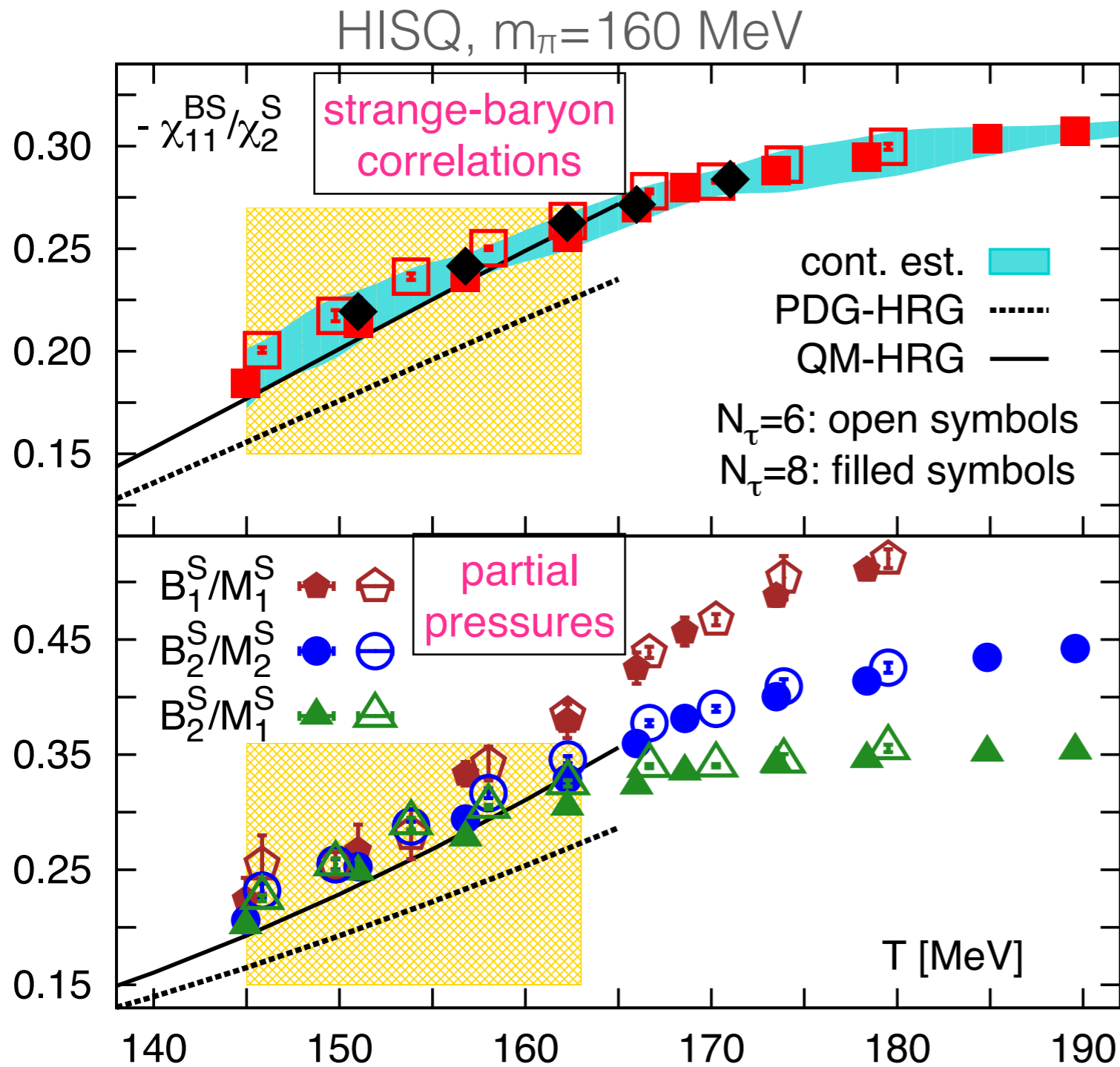
$\chi_{31}^{BS} - \chi_{11}^{BS}$ : receives contributions only from **open strange hadrons**

Deconfinement of open strange hadrons starts to take place in the chiral crossover region

HISQ: Colored points, Bazavov, HTD et al., [BNL-Bielefeld], PRL111(2013)082301  
 stout: Black points, Borsanyi et al., [Wuppertal-Budapest], PRL111(2013)202302



# Indirect evidence of experimentally not yet observed strange states hinted from QCD thermodynamics



**PDG-HRG:** Hadron Resonance Gas model calculations with spectrum from PDG

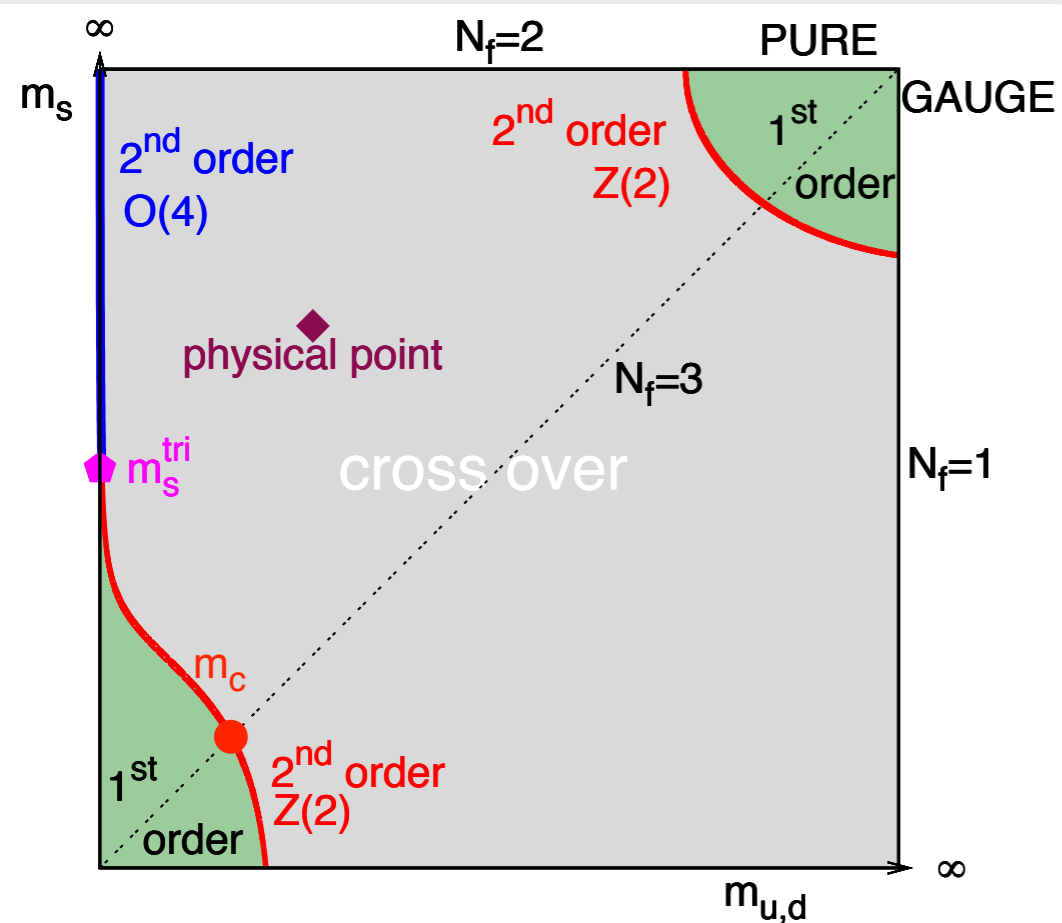
**QM-HRG:** Similar as PDG-HRG but with spectrum from Quark Model

similar findings for charmed states

Bielefeld-BNL-CCNU, PLB737 (2014) 210-215

# QCD phase structure in the quark mass plane

columbia plot, PRL 65(1990)2491



HTD, F. Karsch, S. Mukherjee, 1504.05274

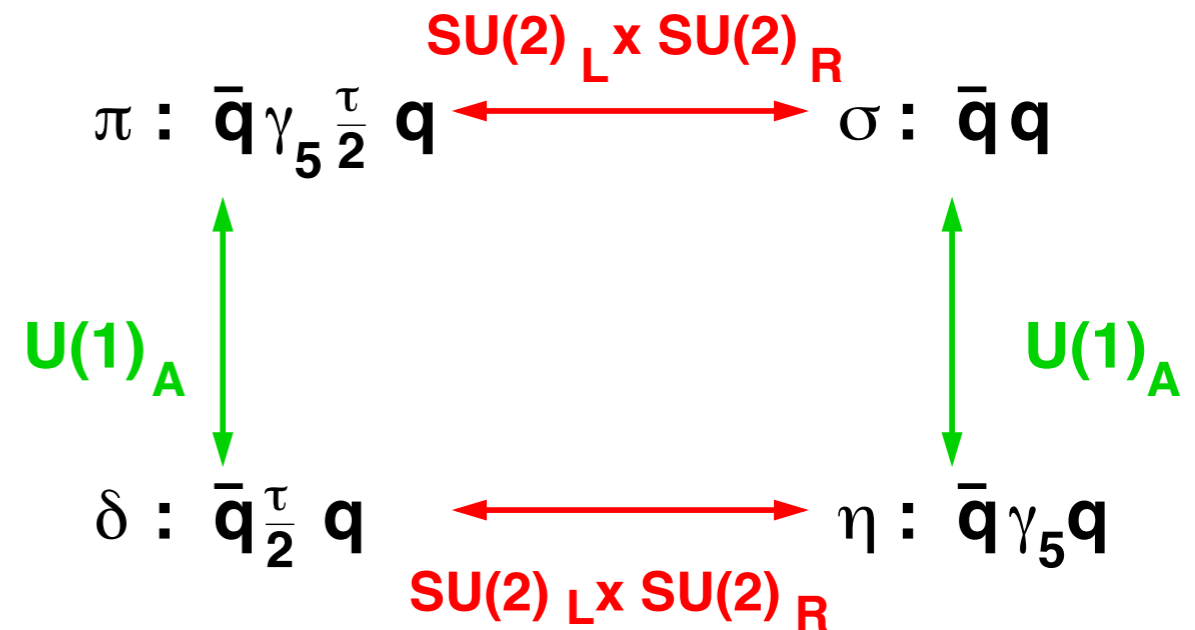
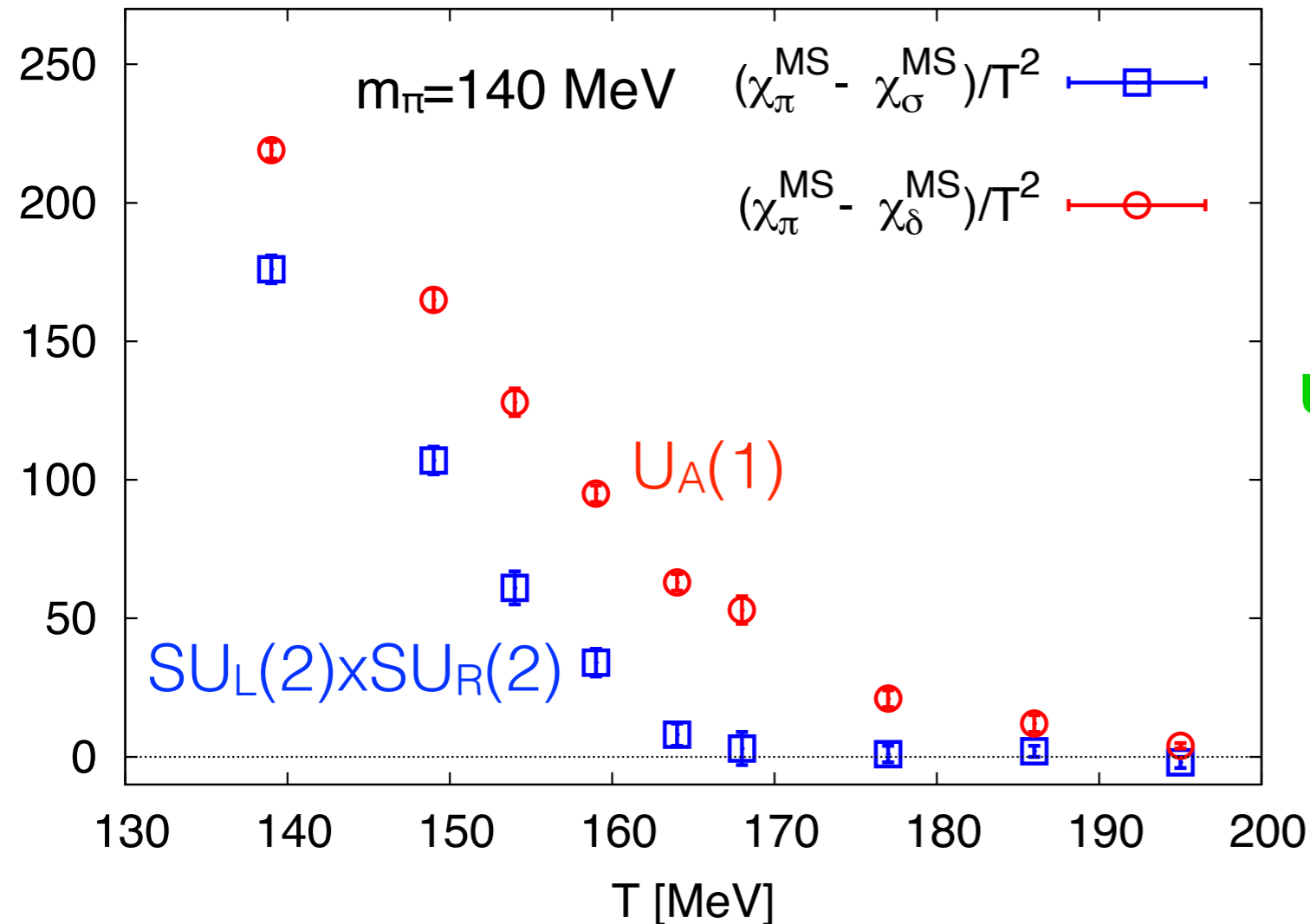
## RG arguments:

- $m_q=0$  or  $\infty$  with  $N_f=3$ : a first order phase transition  
R. Pisarski & F. Wilczek, PRD29 (1984) 338
- Critical lines of second order transition  
  - $N_f=2$ :  $O(4)$  universality class
  - $N_f=3$ :  $Z(2)$  universality class
- $U_A(1)$  symmetry on chiral phase transition restored: 1st or 2nd order ( $U(2)_L \otimes U(2)_R / U(2)_V$ ); broken: 2nd  $O(4)$   
F. Wilczek, JMPA 7(1992) 3911,6951  
K. Rajagopal & F. Wilczek, NPB 399 (1993) 395  
Gavin, Gocksch & Pisarski, PRD 49 (1994) 3079  
Butti, Pelissetto and Vicar, JHEP 08 (2003)029

- fate of the axial  $U(1)$  symmetry at finite  $T$  ?
- The value of tri-critical point ( $m_s^{\text{tri}}$ ) ?
- The location of 2<sup>nd</sup> order  $Z(2)$  lines ?
- The influence of criticalities to the physical point ?

# Fate of chiral symmetries at $T \neq 0$ : $N_f=2+1$ QCD

Domain Wall fermions,  $32^3 \times 8$ ,  $L_s=24, 16$



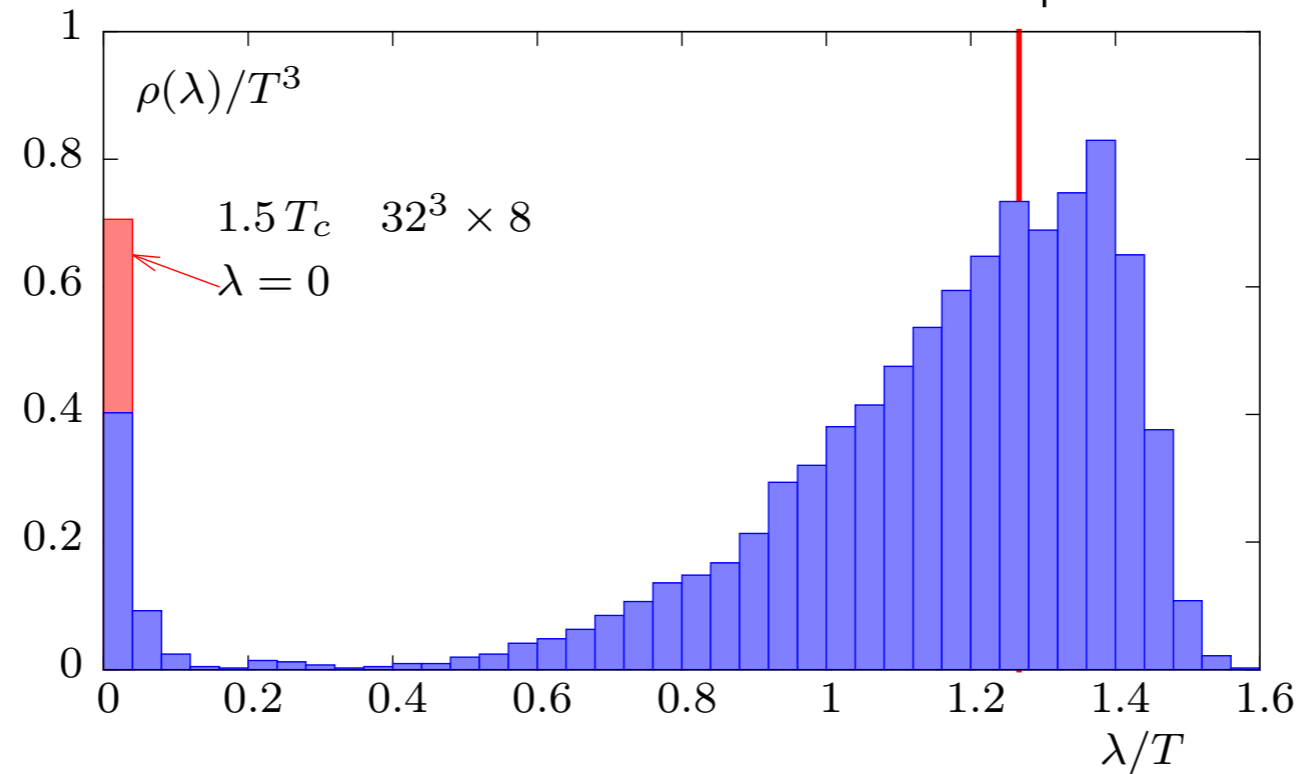
HotQCD, PRL 113 (2014) 082001, PRD 89 (2014) 054514

At the physical point,  $U(1)_A$  does not restore at  $T_{\chi\text{SB}} \sim 170$  MeV,  
remains broken up to  $195$  MeV  $\sim 1.16 T_{\chi\text{SB}}$

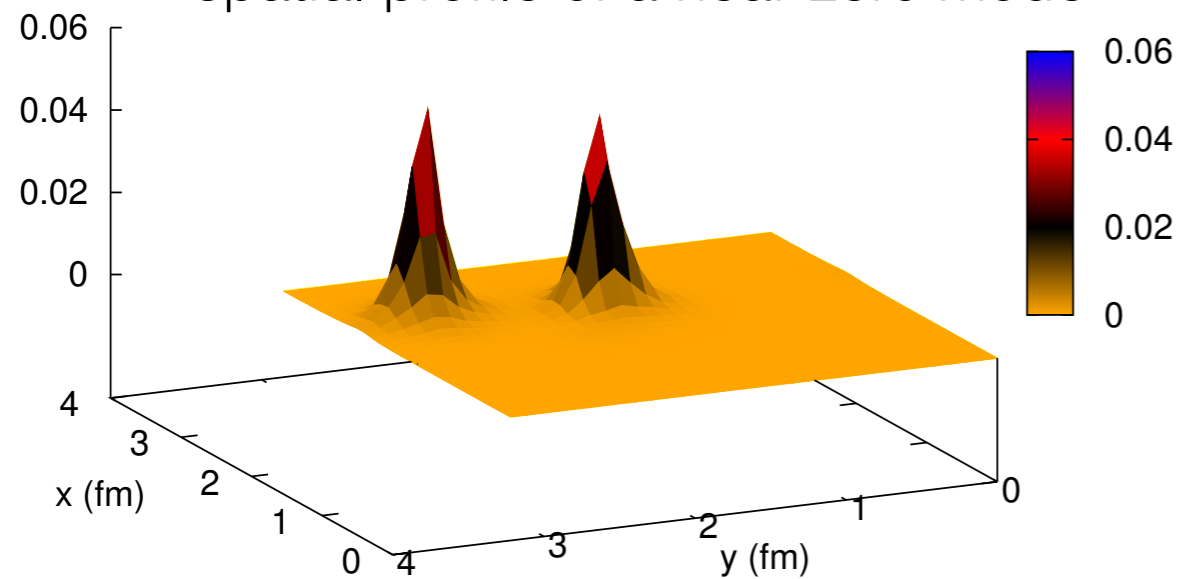
See also H. Fukaya, lattice 2017, Petreczky et al., arXiv:1606.03145,  
Tomiya et al., 1612.01908, Brandt et al., 1608.06882

# Microscopic origin of $U_A(1)$ breaking

accumulation of near-zero modes of the Overlap-Dirac fermion matrix

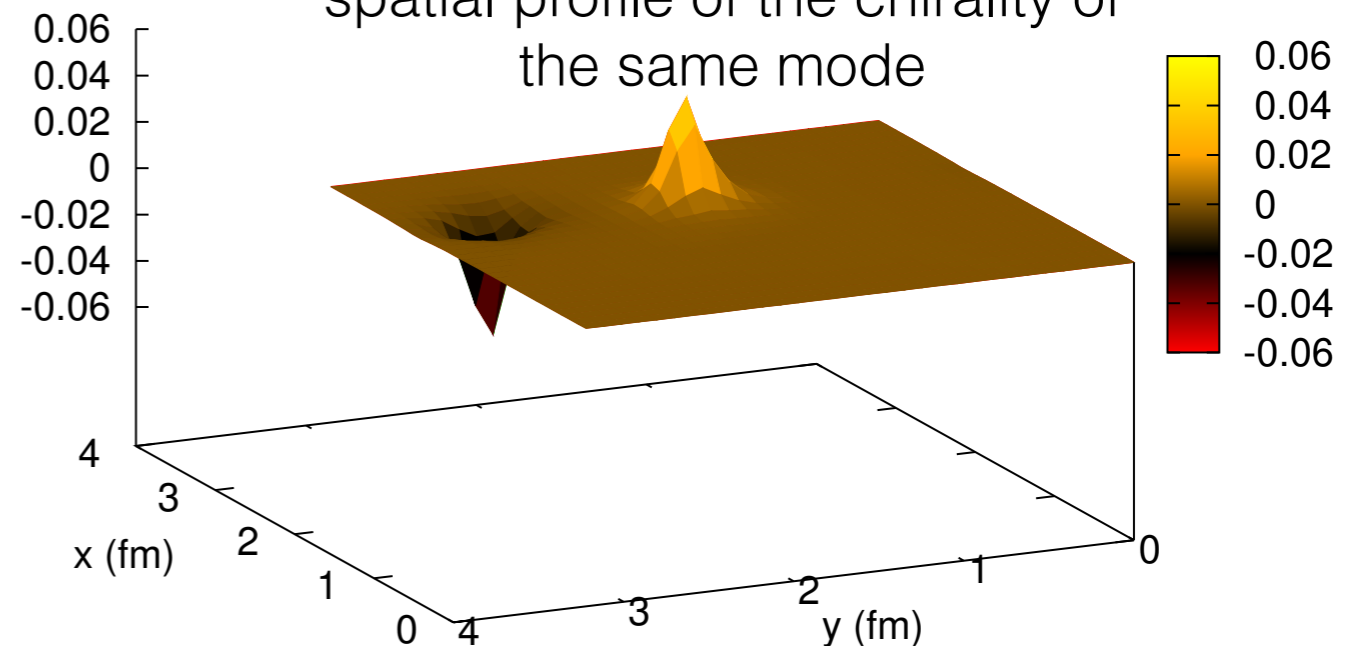


$\psi^+\psi$  spatial profile of a near zero mode

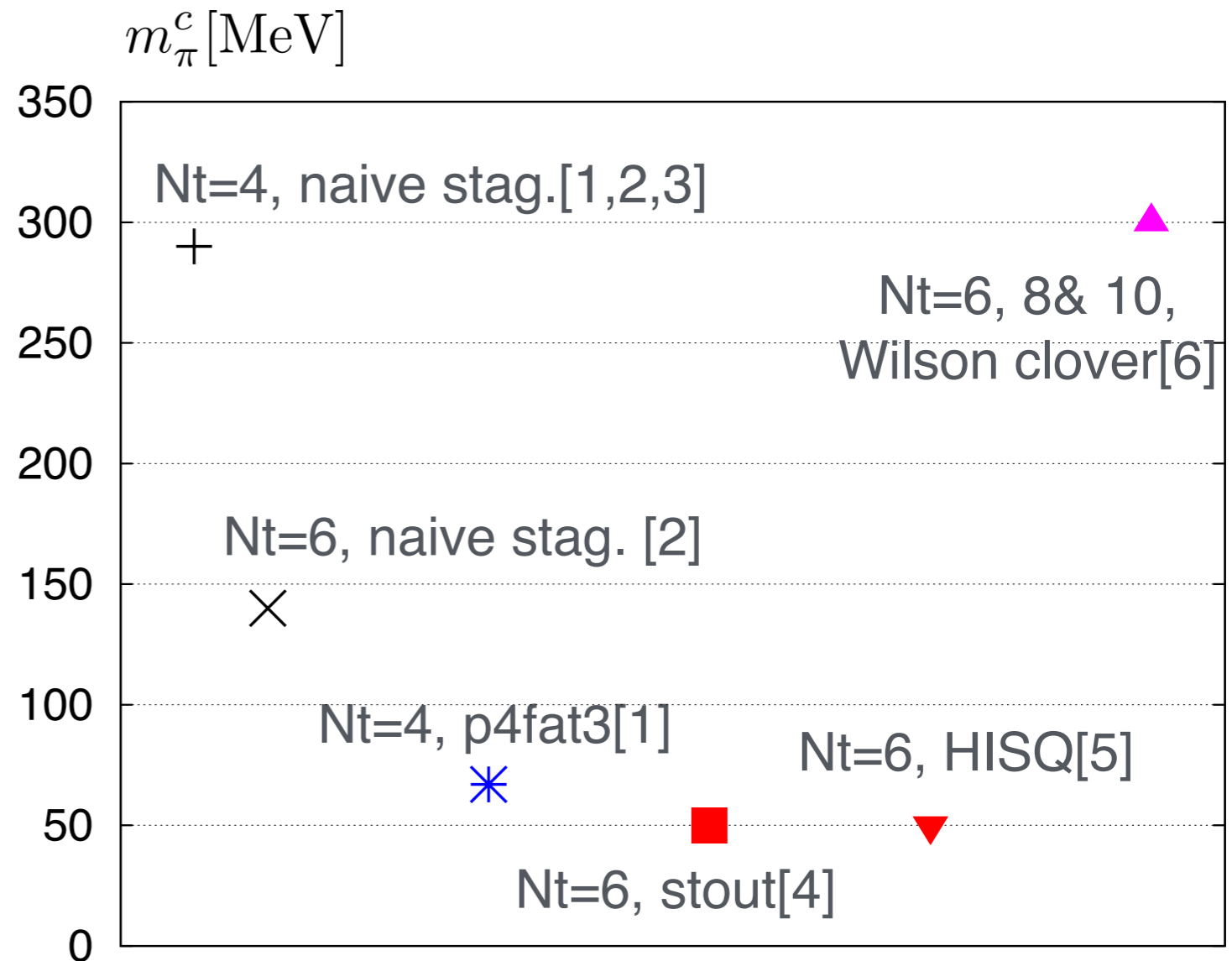
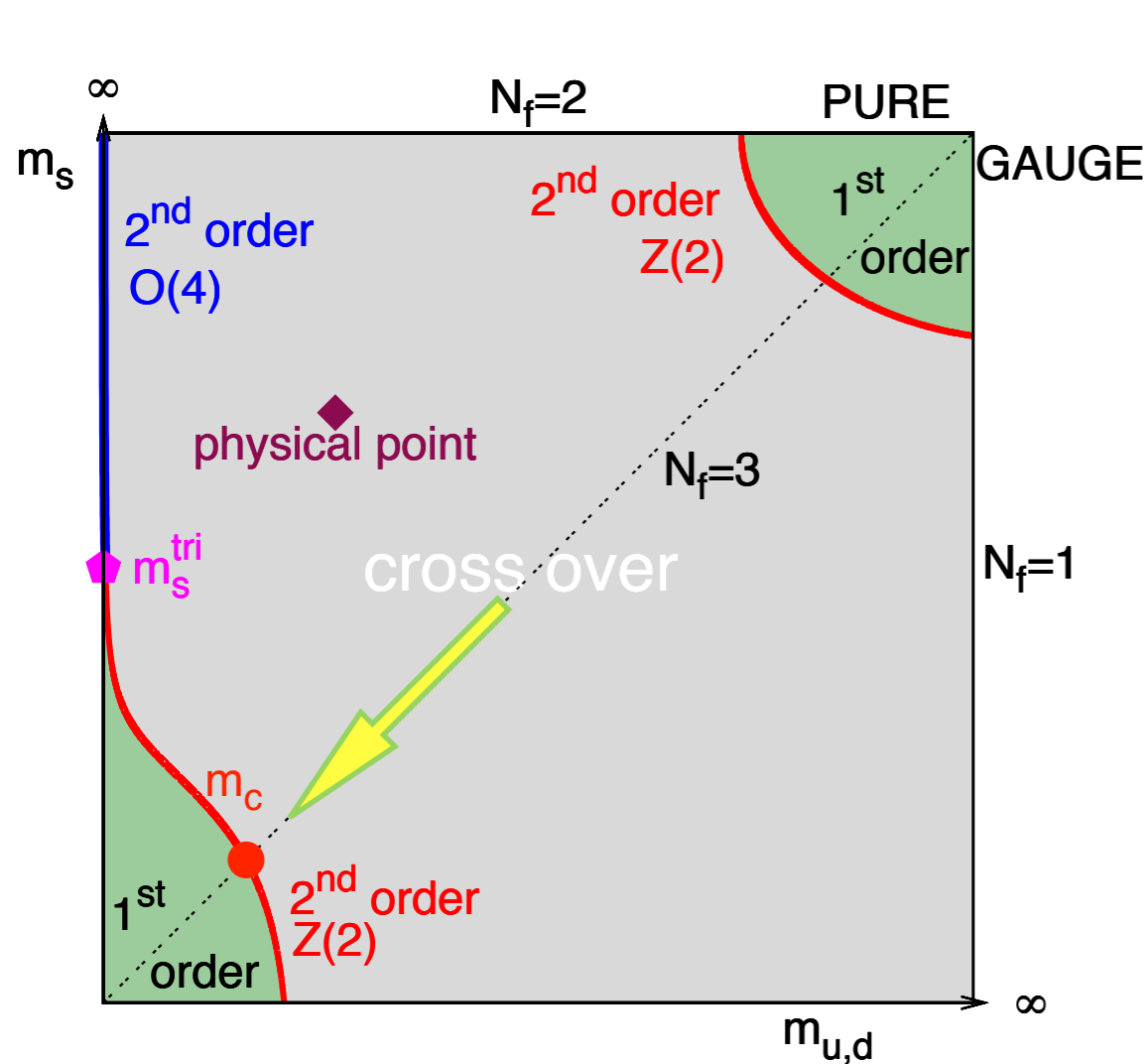


$\psi^+\gamma_5\psi$

spatial profile of the chirality of the same mode



# 1st order chiral phase transition region



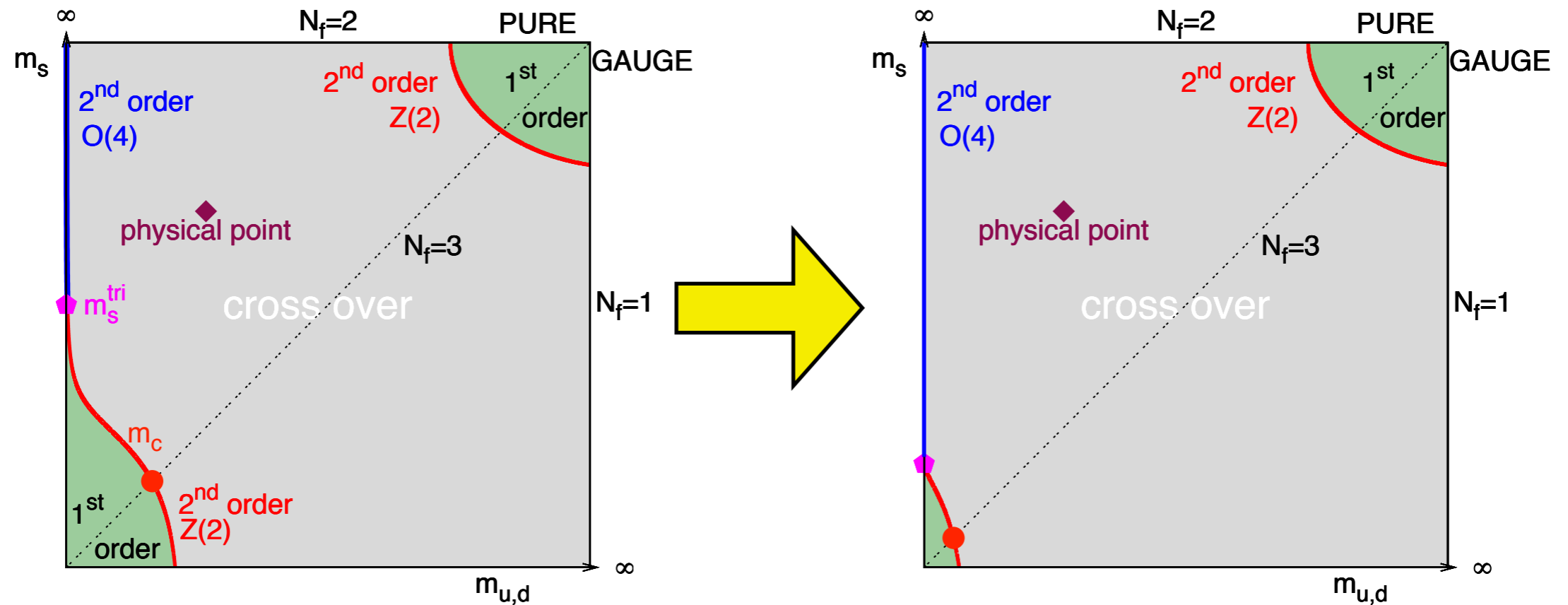
1st order chiral phase transition region shrinks towards the continuum limit

[1]F. Karsch et al., Nucl.Phys.Proc.Suppl. 129 (2004) 614 [2] P. de Forcrand et al, PoS LATTICE2007 (2007) 178

[3]D. Smith & C. Schmidt, Lattice 2011 [4]G. Endrodi et al., PoS LAT2007 (2007) 228

[5] Bielefeld-BNL-CCNU, Phys.Rev. D 95 (2017) no.7, 074505 [6]Y. Nakamura, Lattice 15',PRD92 (2015) no.11, 114511

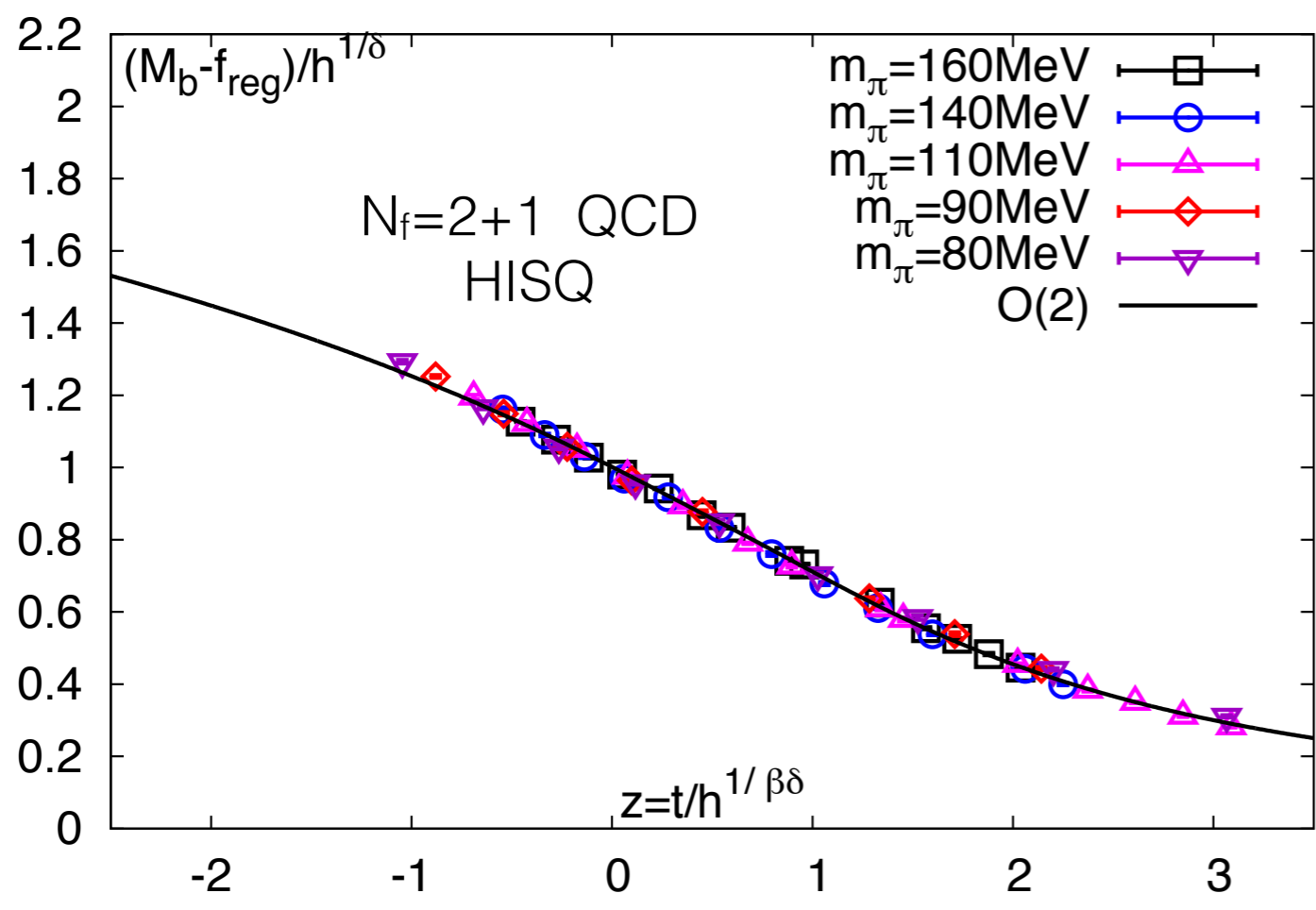
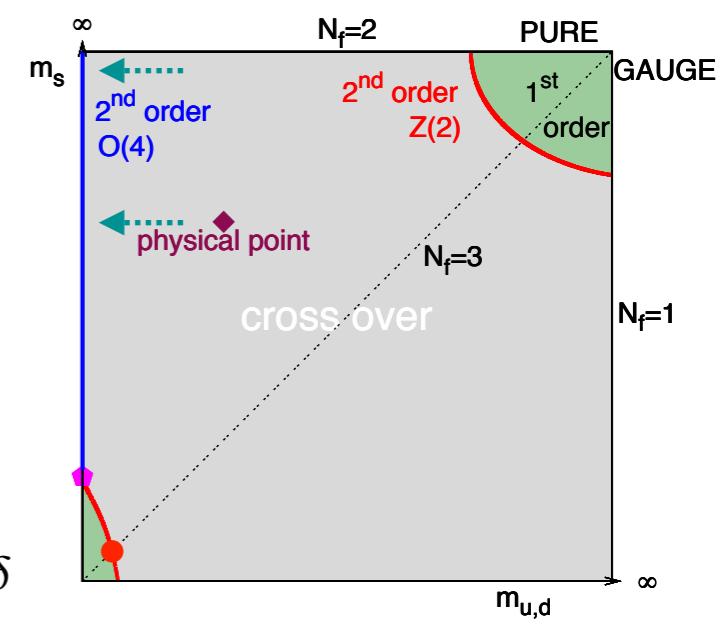
# Chiral phase transition region in $N_f=3$ QCD



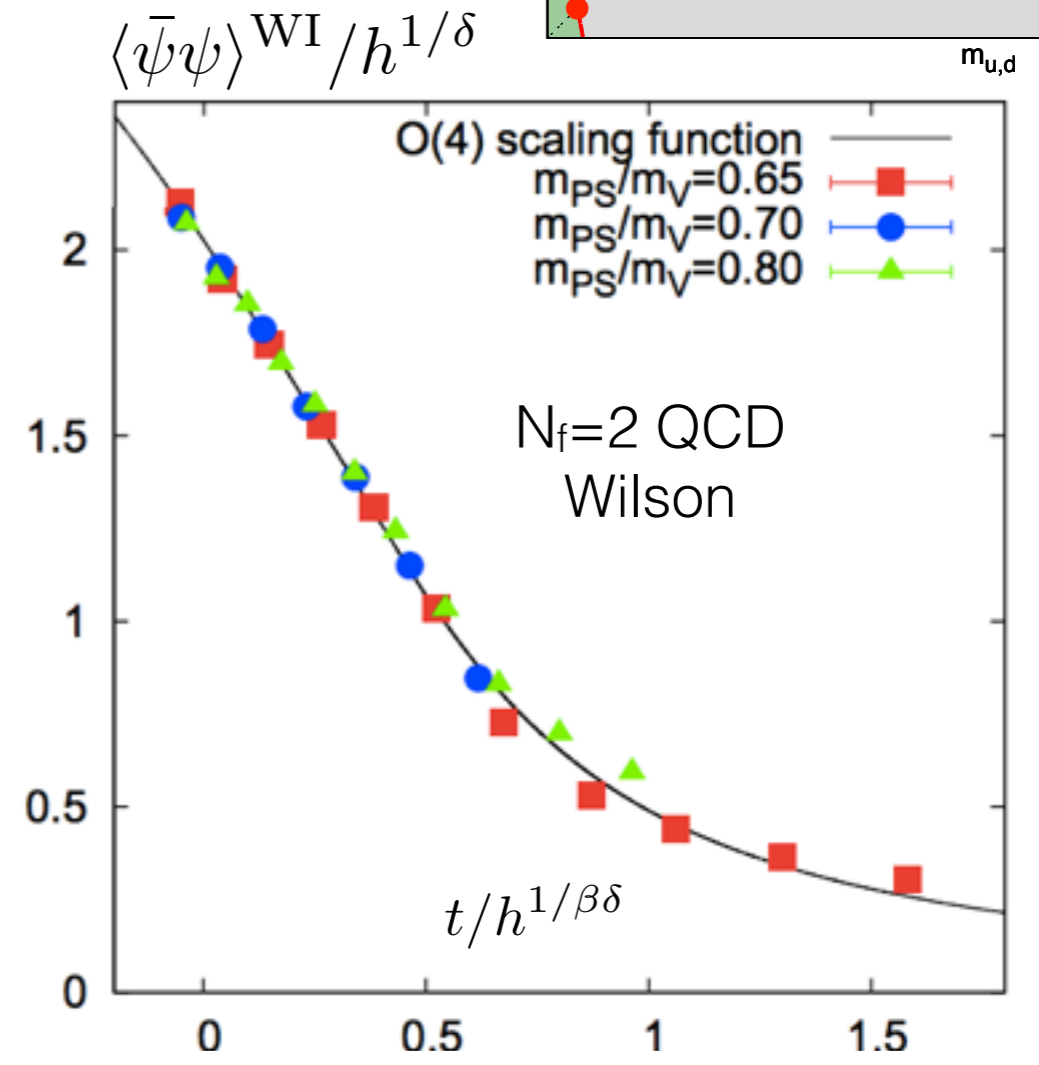
1st order chiral phase transition seems to be not much relevant to thermodynamics at the physical point

How about the 2nd order  $O(4)$  transition line?

# Universal behavior of chiral phase transition in $N_f=2+1$ & 2 QCD at $\mu_B=0$



S.T. Li, [Bielefeld-BNL-CCNU], arXiv:1702.01294

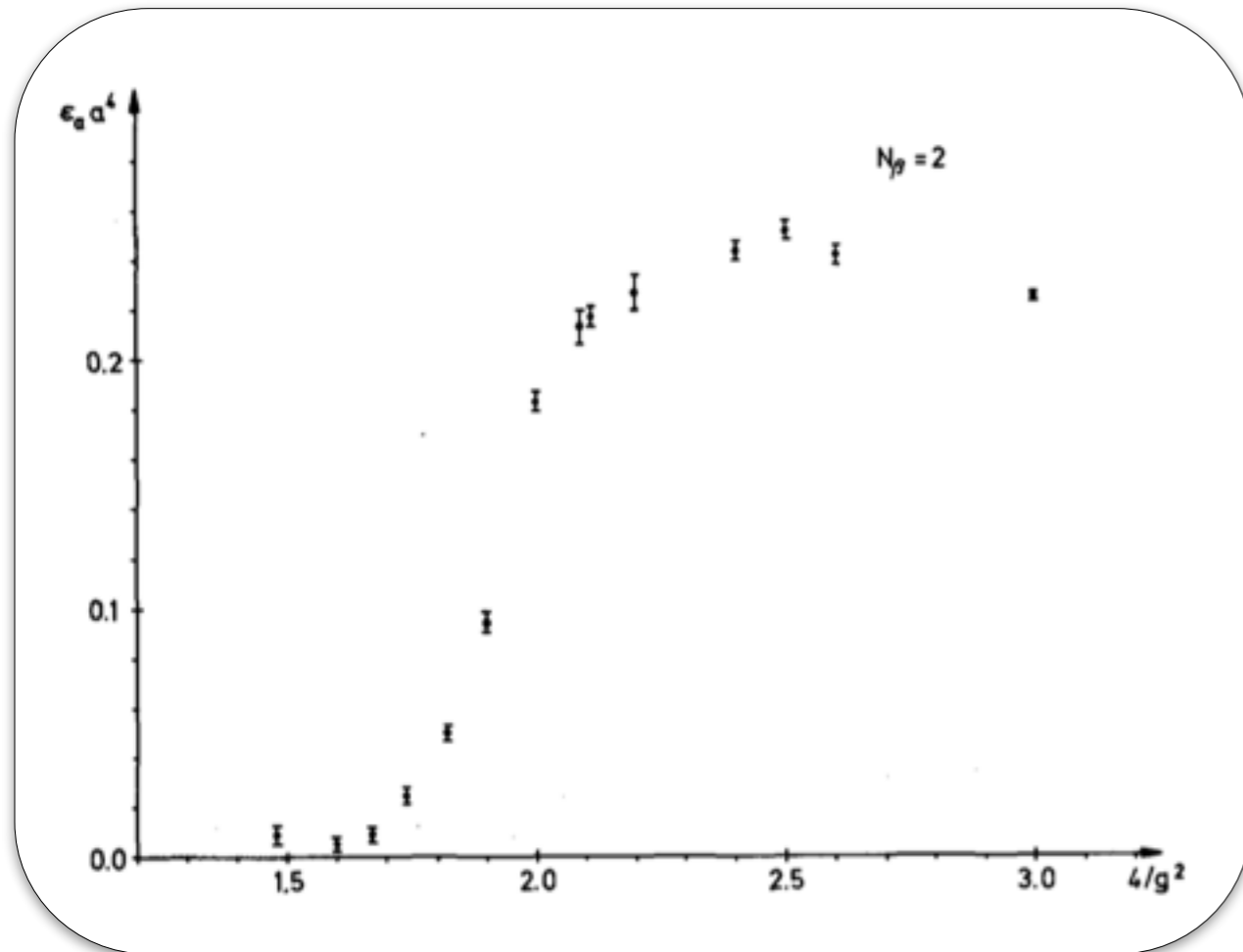


T. Umeda, [WHOT], arXiv:1612.09449

Good evidence of  $O(N)$  scaling for chiral phase transition in  $N_f=2+1$  and 2 QCD

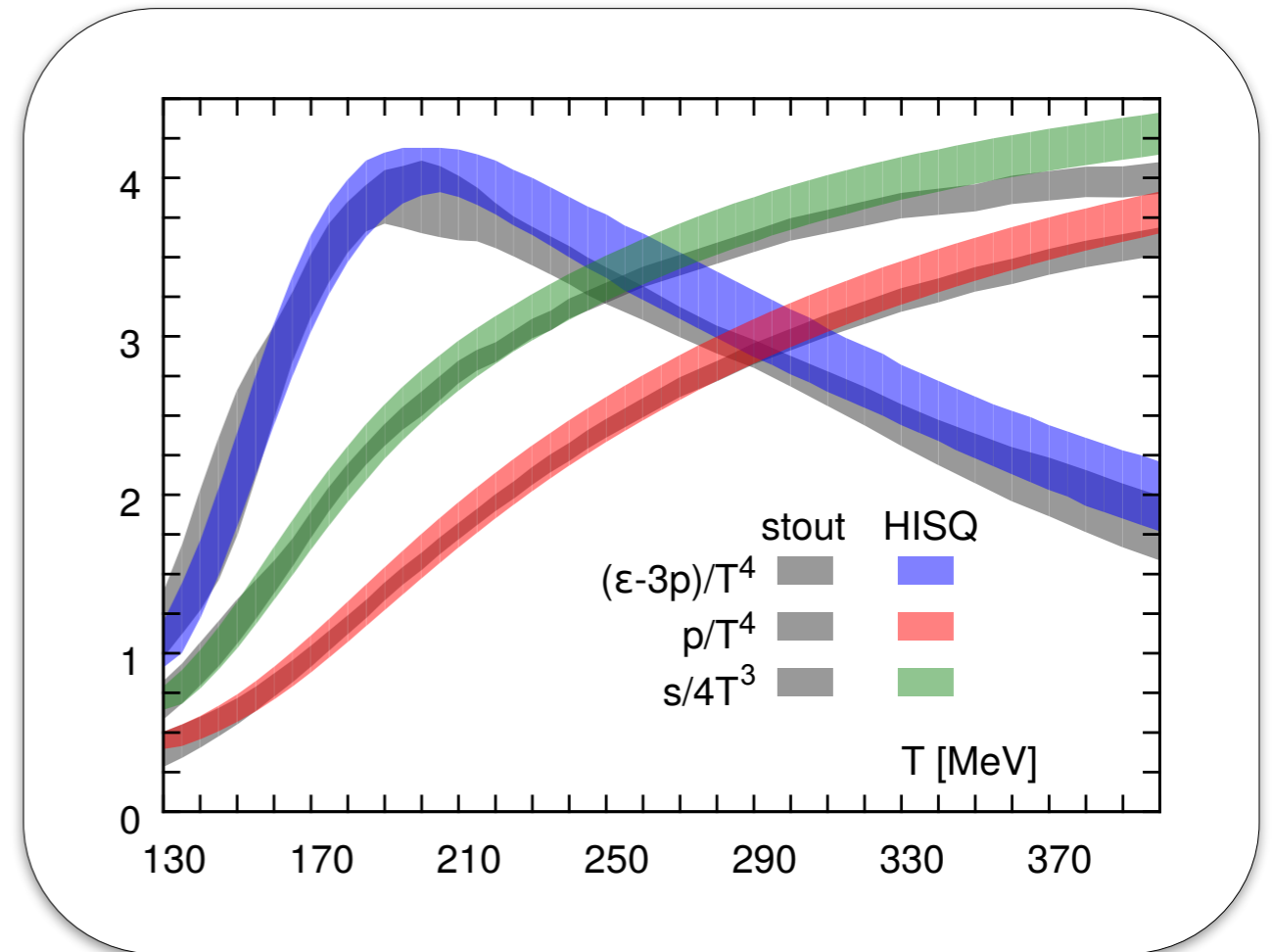
# Lattice QCD calculation of EoS at $\mu_B = 0$

SU(2) pure gauge  
at a finite lattice cutoff of  $Nt=2$



J. Engels, F. Karsch, H. Satz, I. Montvay  
Phys. Lett. B 101 (1981) 89-94

$N_f=2+1$ , physical pion mass  
continuum extrapolated



HotQCD, PRD 90 (2014) 094503  
Wuppertal-Budapest, Phys. Lett. B730 (2014) 99

- 📍 First lattice QCD calculation of EoS was done in 1981
- 📍 Only recently a conclusive QCD EoS at  $\mu_B=0$  is obtained



# QCD equation of state at $\mu_B > 0$

• Sign problem; several approaches exist: Reweighting, imaginary  $\mu_B$ , complex Langevin, Lefschetz thimbles...

• Taylor Expansion Method: expansion in  $\mu_B/T$

Allton et al., PRD66 (2002) 074507

Gavai & Gupta et al., PRD68 (2003) 034506

$$\frac{p}{T^4} = \frac{1}{VT^3} \ln \mathcal{Z}(T, V, \hat{\mu}_u, \hat{\mu}_d, \hat{\mu}_s) = \sum_{i,j,k=0}^{\infty} \frac{\chi_{ijk}^{BQS}}{i!j!k!} \left(\frac{\mu_B}{T}\right)^i \left(\frac{\mu_Q}{T}\right)^j \left(\frac{\mu_S}{T}\right)^k$$

$$\chi_{ijk}^{BQS} \equiv \chi_{ijk}^{BQS}(T) = \frac{1}{VT^3} \left. \frac{\partial P(T, \hat{\mu})/T^4}{\partial \hat{\mu}_B^i \partial \hat{\mu}_Q^j \partial \hat{\mu}_S^k} \right|_{\hat{\mu}=0}$$

$$\frac{\epsilon - 3p}{T^4} = T \frac{\partial P/T^4}{\partial T} = \sum_{i,j,k=0}^{\infty} \frac{T d\chi_{ijk}^{BQS}/dT}{i!j!k!} \left(\frac{\mu_B}{T}\right)^i \left(\frac{\mu_Q}{T}\right)^j \left(\frac{\mu_S}{T}\right)^k$$

• Imaginary potential: MC simulation with Imaginary  $-i\mu_B$ ; analytic continuation to real  $\mu_B$  needed

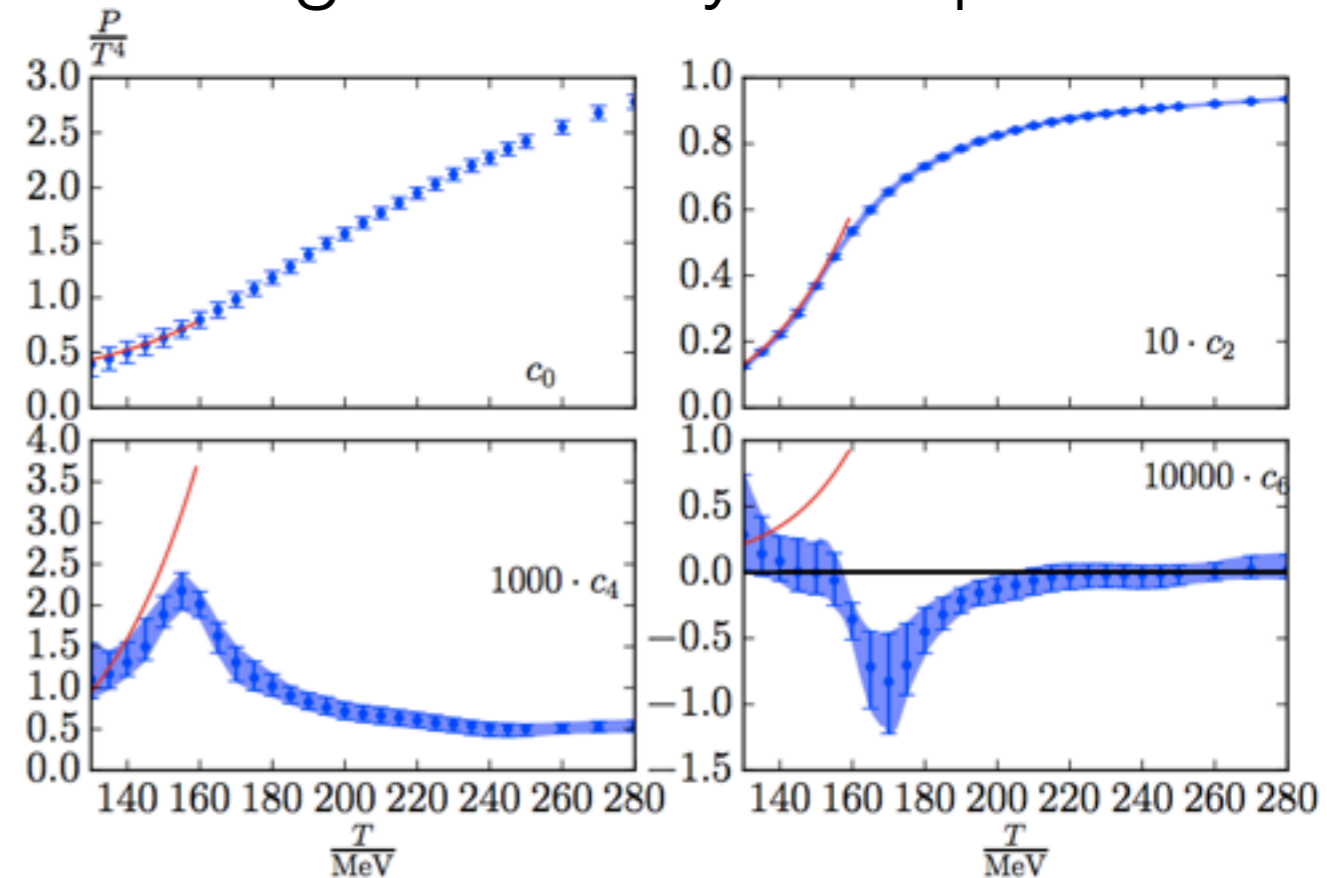
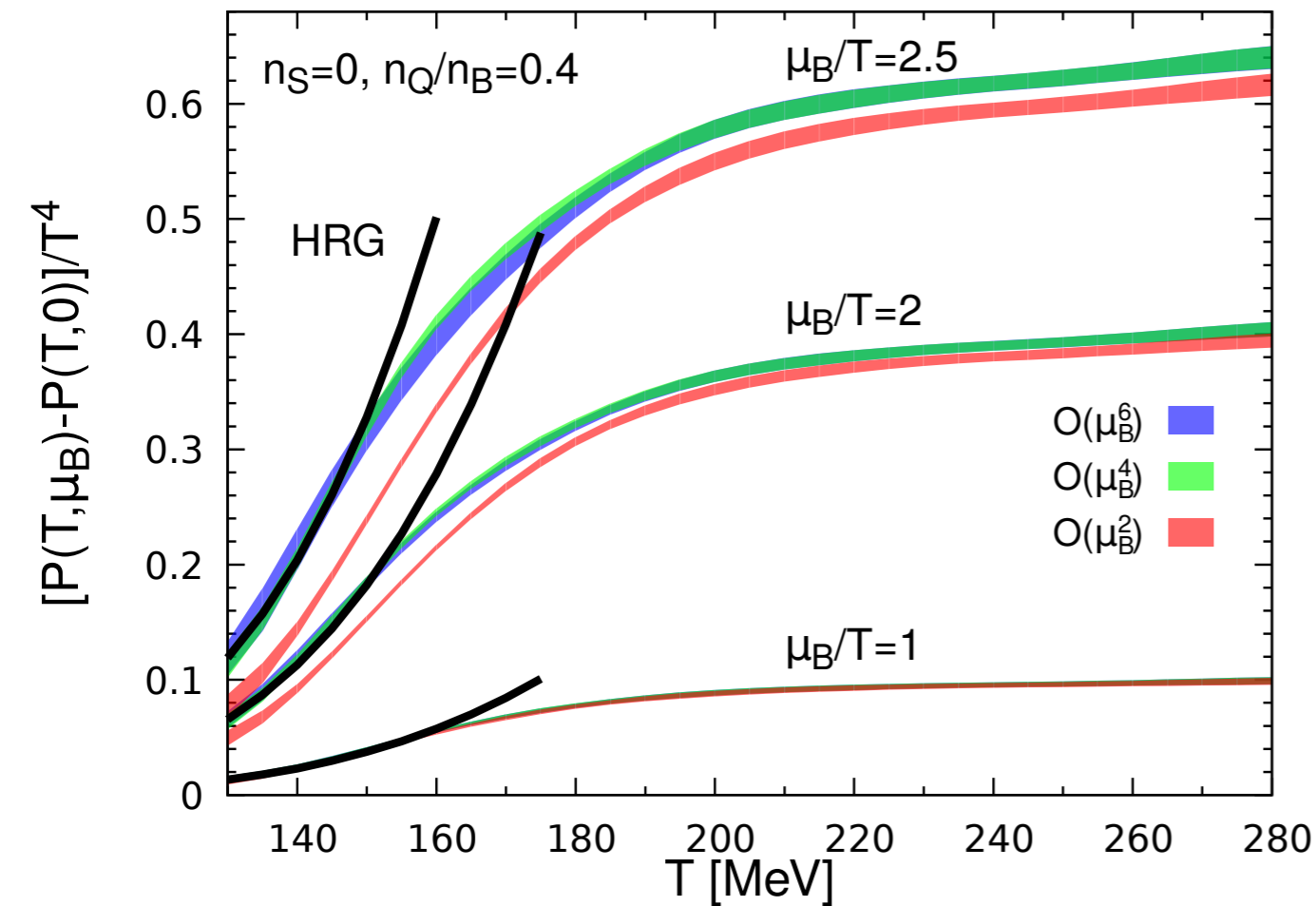
de Forcrand & Philipsen, Nucl.Phys. B642 (2002) 290-306

D'Elia & Lombardo, Phys.Rev. D67 (2003) 014505

# QCD Equation of State at nonzero $\mu_B$

Taylor expansion

Img. mu + Taylor expansion



Bielefeld-BNL-CCNU, Phys.Rev. D95 (2017) no.5, 054504

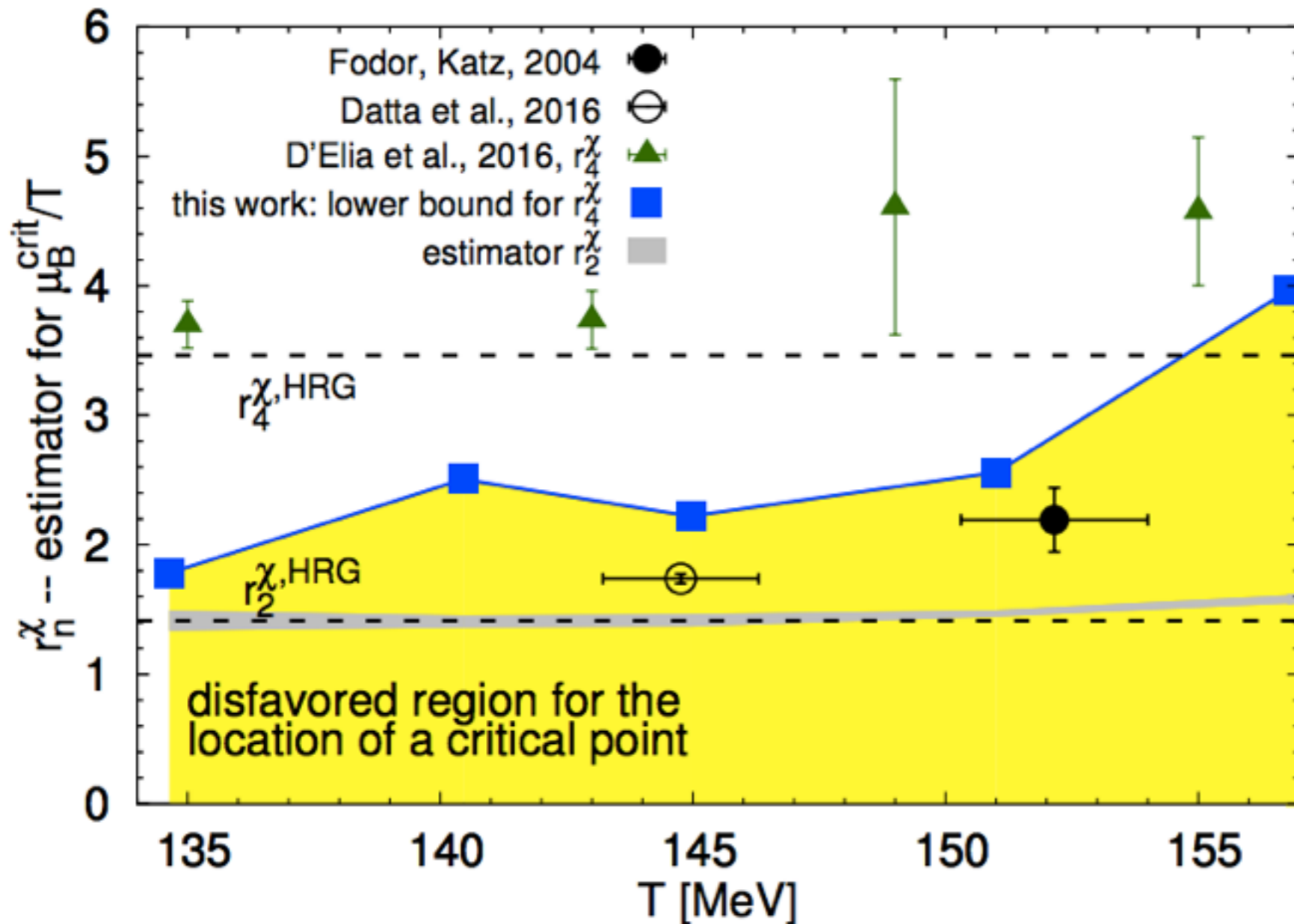
Wuppertal-Budapest-Houston:  
EPJ Web Conf. 137 (2017) 07008

The EoS is well under control at  $\mu_B/T \lesssim 2$  or  $\sqrt{s_{NN}} \gtrsim 12$  GeV

Consistent results obtained from two approaches & discretization schemes

# Location of critical point: strongly disfavored at $\mu_B/T \lesssim 2$

$$\text{radius of convergence} = \lim_{n \rightarrow \infty} r_{2n}^\chi = \lim_{n \rightarrow \infty} \left| \frac{2n(2n-1)\chi_{2n}^B}{\chi_{2n+2}^B} \right|^{1/2}$$



HISQ + Taylor Exp. (this work):  
Bielefeld-BNL-CCNU,  
PRD 95 (2017) no.5, 054504

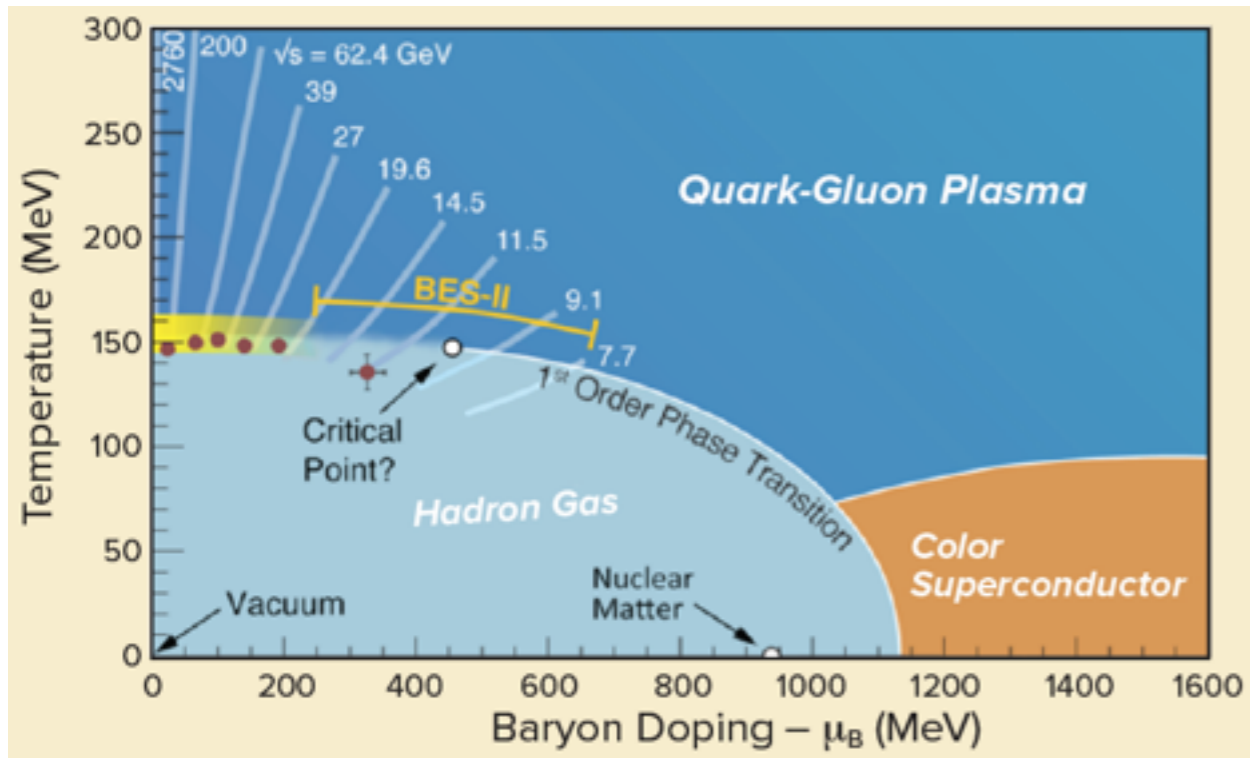
stout + Img. mu:  
D'Elia et al., PRD 95 (2017) 094503

unimproved staggered + Taylor Exp.:  
Datta et al., PRD 95 (2017) 054512

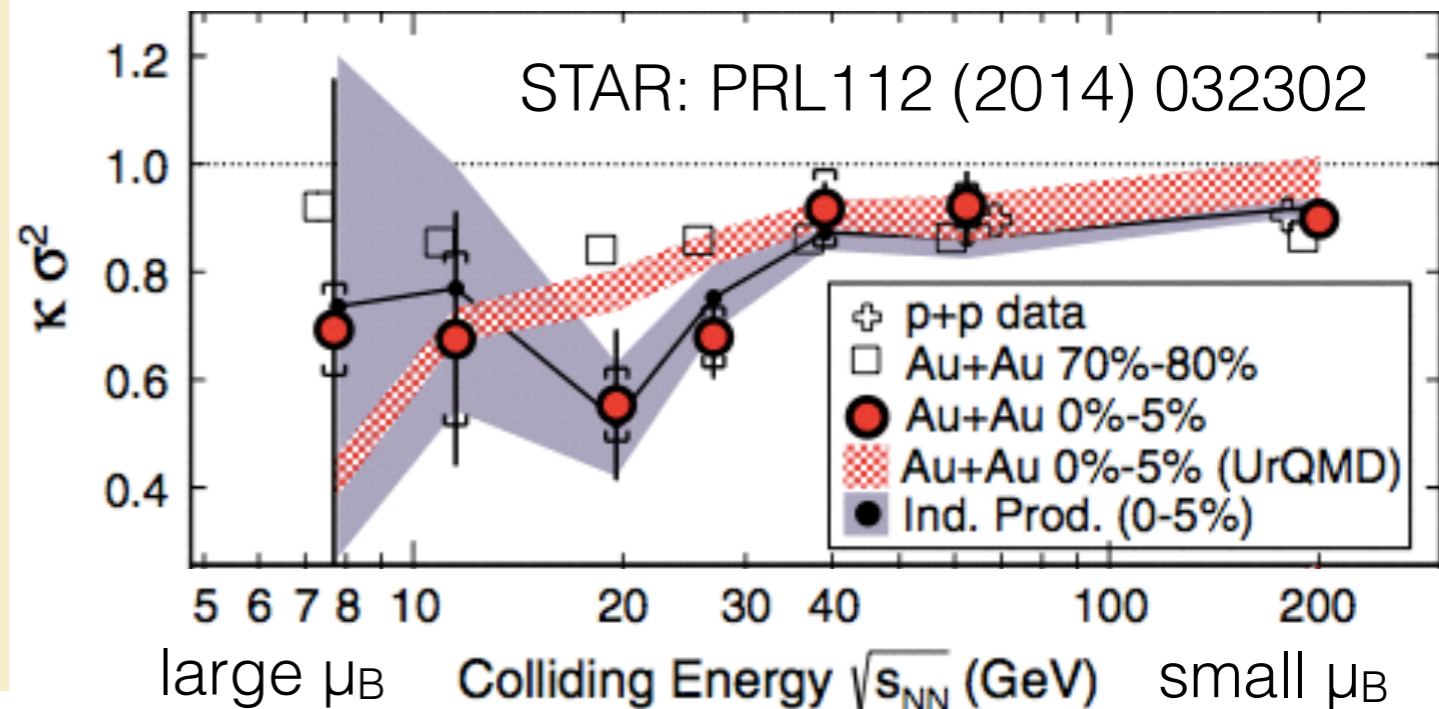
unimproved staggered + Reweighting:  
Fodor and Katz, JHEP 0404 (2004) 050

# Search for critical point in HIC

Beam Energy Scan(BES) @RHIC



Ratio of the 4th to 2nd order proton number fluctuations



Can this non-monotonic behavior be understood in terms of the QCD thermodynamics in equilibrium?

What is the relation of this intriguing phenomenon to the critical behavior of QCD phase transition?

# Explore the QCD phase diagram through fluctuations of conserved charges

Comparison of experimentally measured higher order cumulants of conserved charges to those from LQCD, e.g.:

$$\frac{M_Q(\sqrt{s})}{\sigma_Q^2(\sqrt{s})} = \frac{\langle N_Q \rangle}{\langle (\delta N_Q)^2 \rangle} = \frac{\chi_1^Q(T, \mu_B)}{\chi_2^Q(T, \mu_B)} = R_{12}^Q(T, \mu_B)$$

$$\frac{S_Q(\sqrt{s}) \sigma_Q^3(\sqrt{s})}{M_Q(\sqrt{s})} = \frac{\langle (\delta N_Q)^3 \rangle}{\langle N_Q \rangle} = \frac{\chi_3^Q(T, \mu_B)}{\chi_1^Q(T, \mu_B)} = R_{31}^Q(T, \mu_B)$$

**HIC**

mean:  $M_Q$   
 variance:  $\sigma_Q^2$   
 skewness:  $S_Q$   
 kurtosis:  $K_Q$

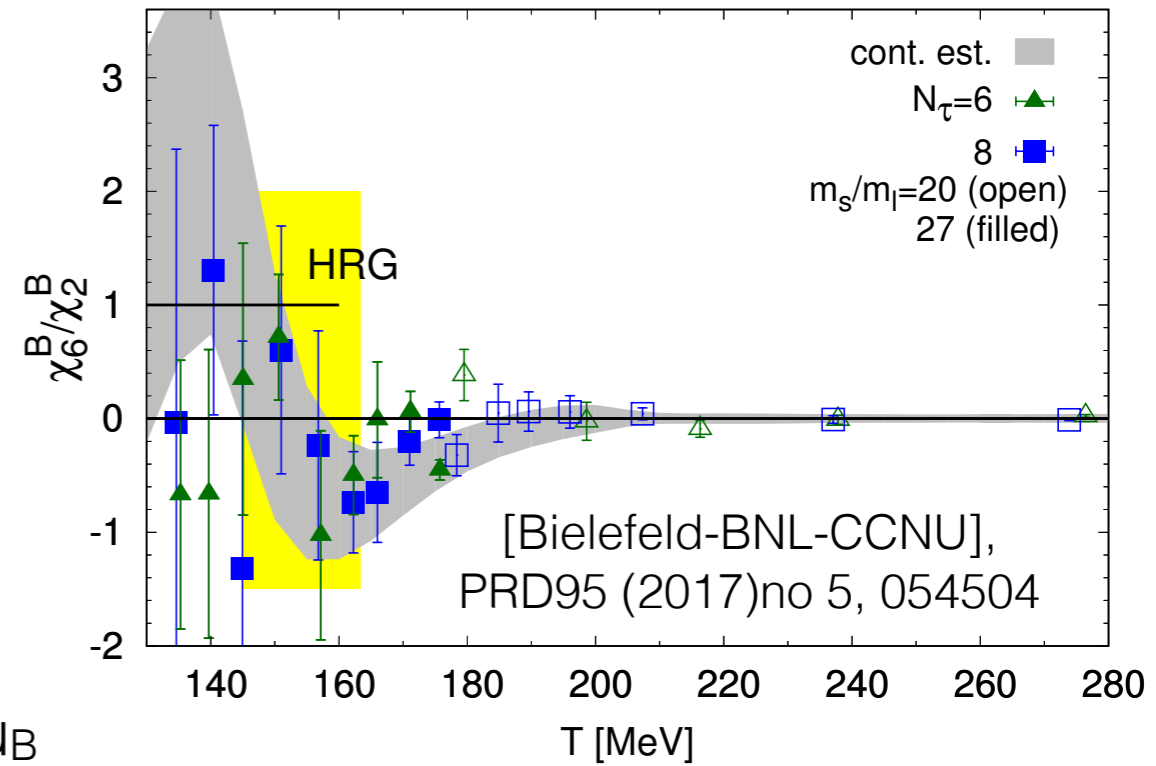
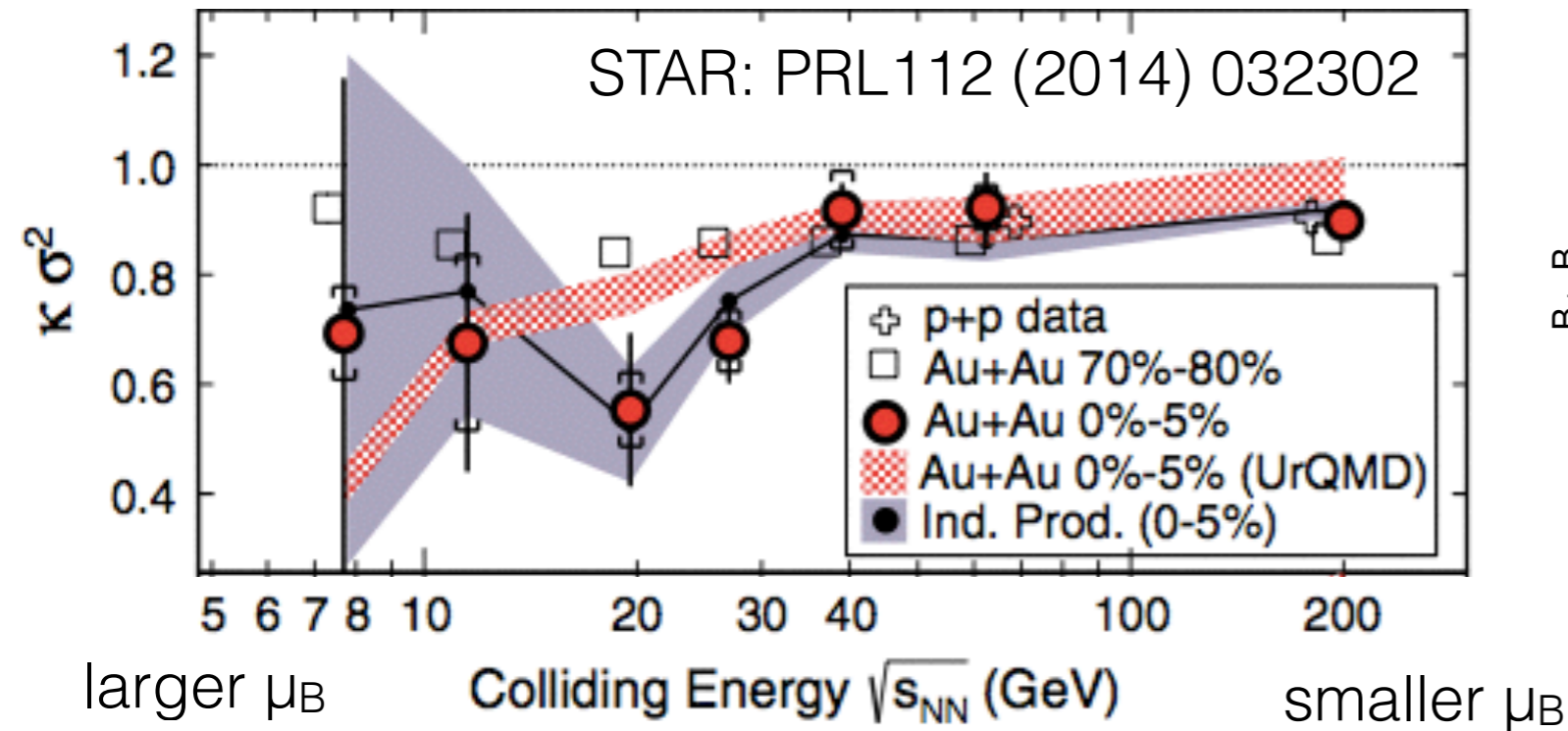
**LQCD**

**generalized susceptibilities**

$$\chi_n^Q(T, \vec{\mu}) = \frac{1}{VT^3} \frac{\partial^n \ln Z(T, \vec{\mu})}{\partial (\mu_Q/T)^n}$$

# Cumulant ratios of proton (baryon) fluctuations: STAR v.s. Lattice

Ratio of the 4th to 2nd order proton number fluctuations



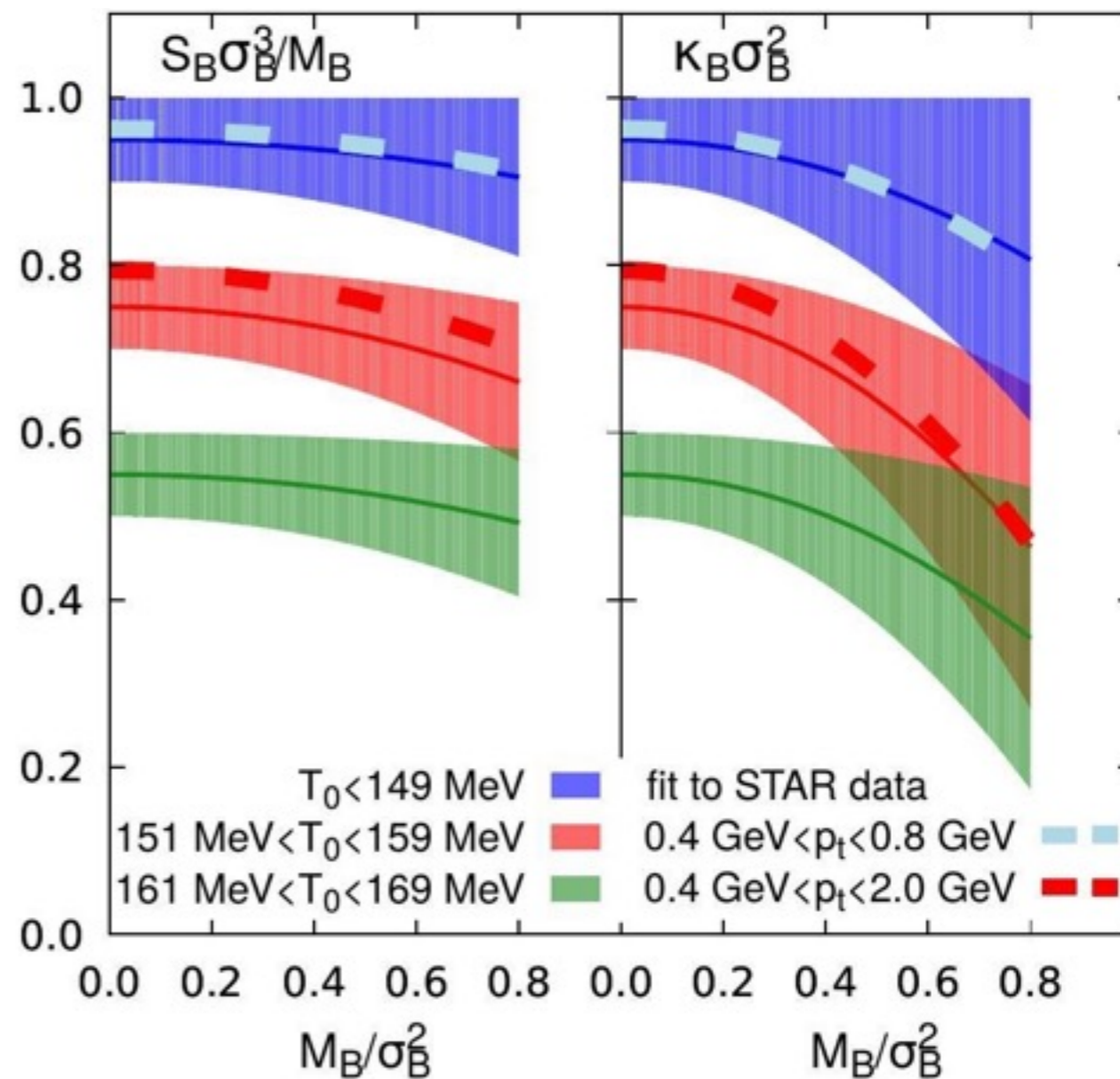
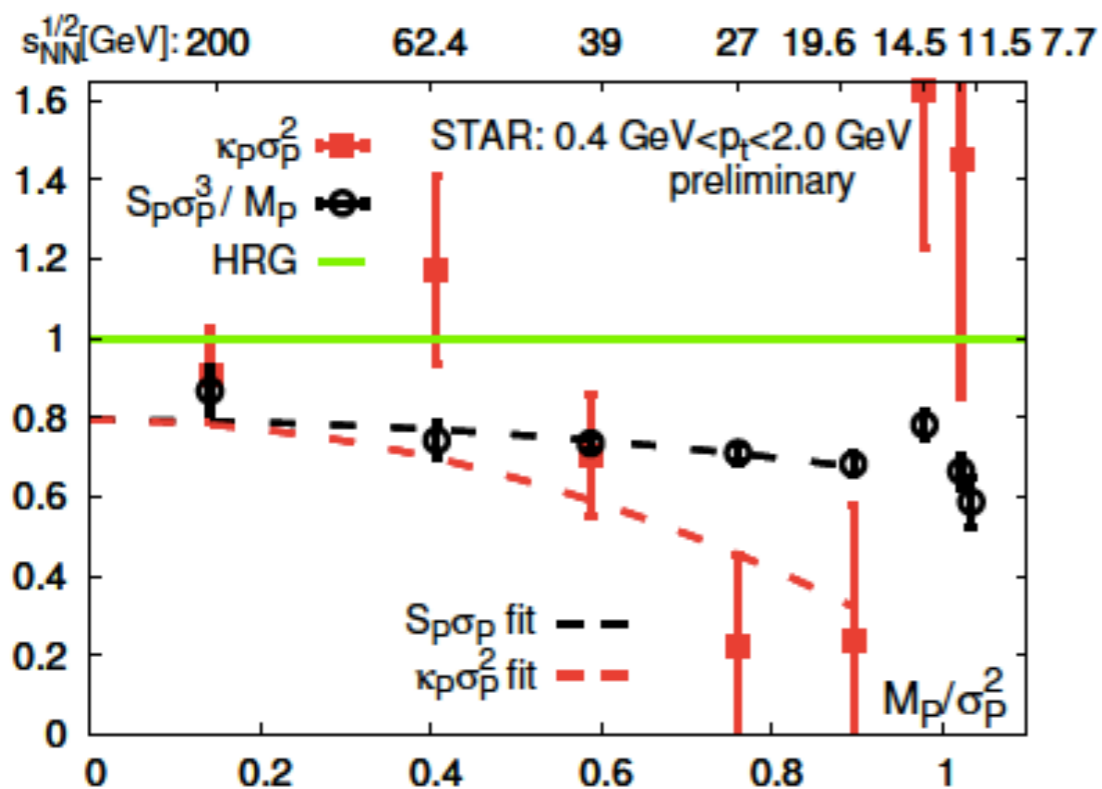
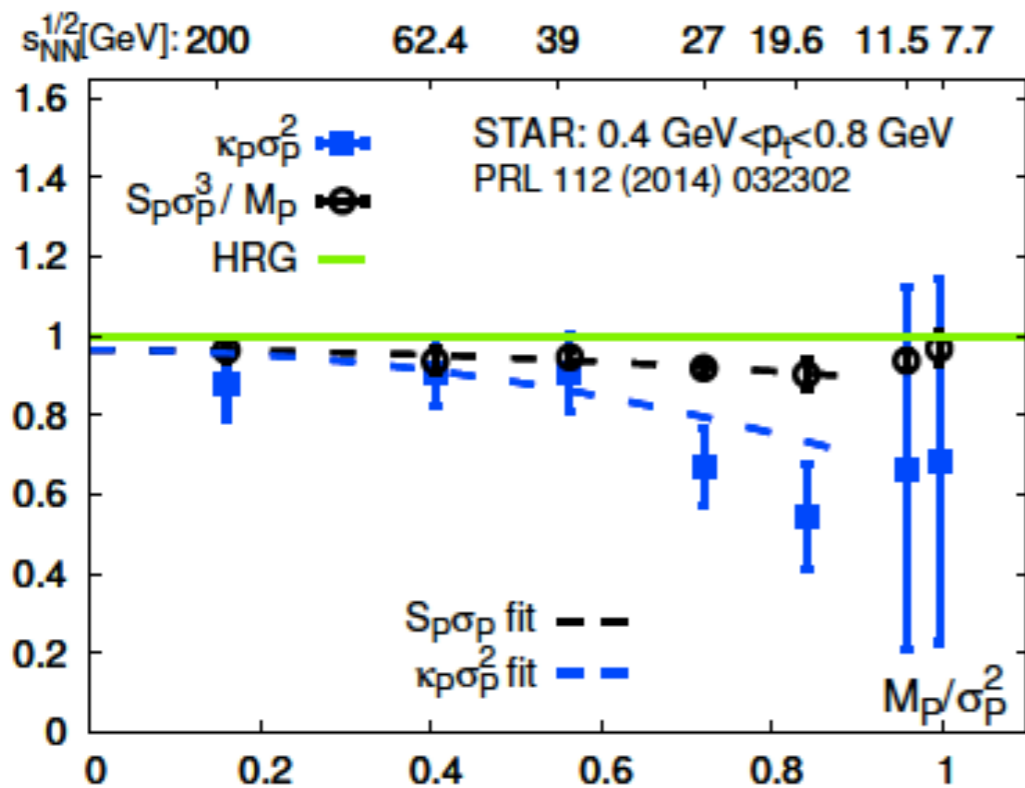
$$(\kappa \sigma^2)_B = \frac{\chi_{4,\mu}^B}{\chi_{2,\mu}^B} = \frac{\chi_4^B}{\chi_2^B} \left[ 1 + \left( \frac{\chi_6^B}{\chi_4^B} - \frac{\chi_4^B}{\chi_2^B} \right) \left( \frac{\mu_B}{T} \right)^2 + \dots \right]$$

HRG:  $\chi_6^B / \chi_4^B = \chi_4^B / \chi_2^B = 1$ , O(4) & LQCD:  $\chi_6^B / \chi_2^B < 0$ , at  $T \sim T_c$

$\sqrt{s_{NN}} \gtrsim 20$  GeV:

$\kappa \sigma^2$  is consistent with QCD in equilibrium

# Cumulant ratios of proton (baryon) fluctuations: STAR v.s. Lattice

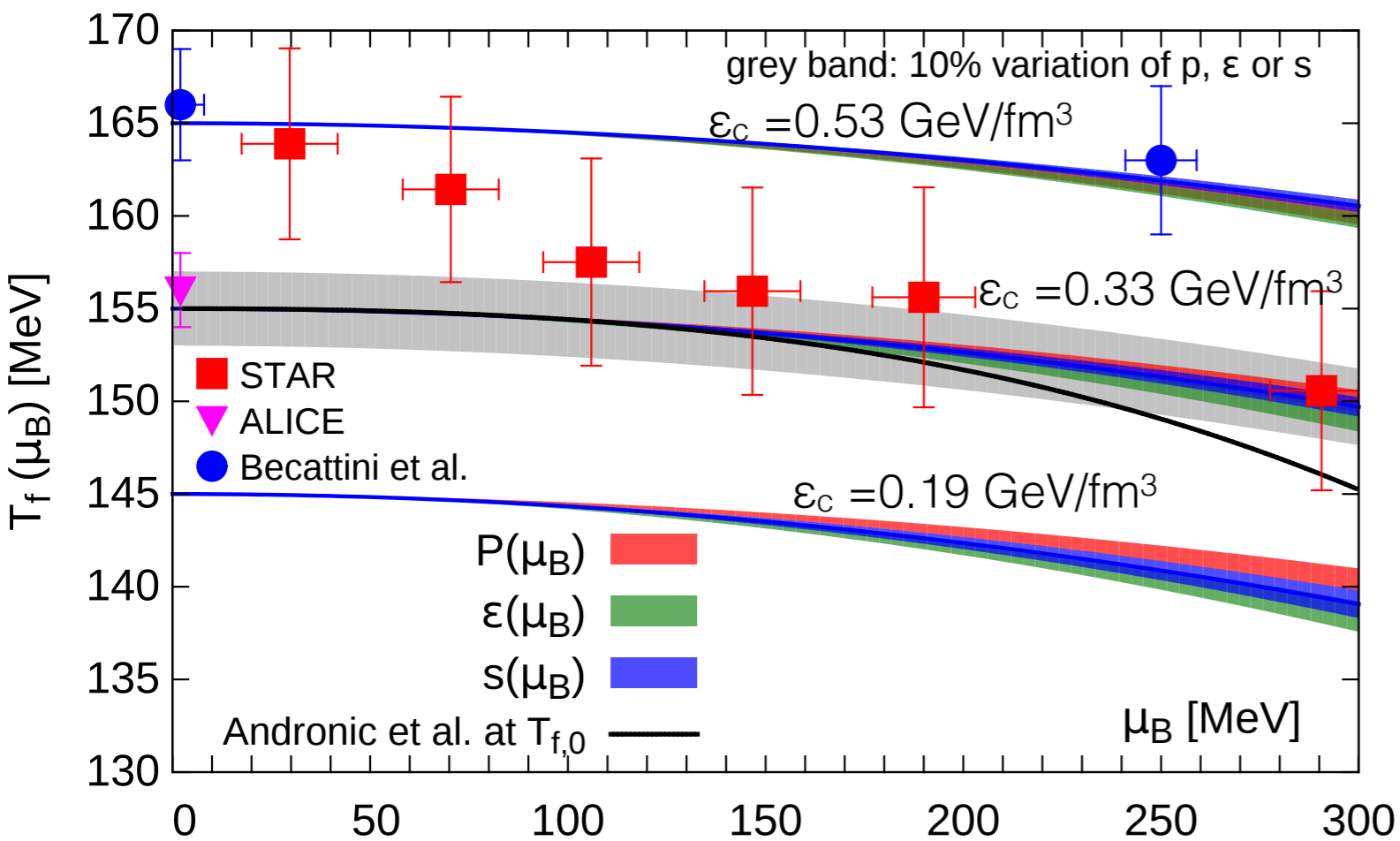


$$T_f(0) = 153 \pm 5 \text{ MeV}$$

C. Schmidt, CPOD 2017,  
Bazavov et al., [HotQCD] in preparation

# Line of constant physics to $O(\hat{\mu}_B^4)$ and freeze-out

Parameterization:  $T(\mu_B) = T(0)(1 - \kappa_2 \hat{\mu}_B^2 + \mathcal{O}(\hat{\mu}_B^4))$



Bielefeld-BNL-CCNU, Phys.Rev. D95 (2017) no.5, 054504

curvature at constant  $b$ :

$$0.006 \leq \kappa_2^b \leq 0.012, \quad b = P, \epsilon, s$$

Bielefeld-BNL-CCNU, PRD95 (2017) no.5, 054504

curvature of freeze-out line:

$$\kappa_2^f \lesssim 0.011$$

Bielefeld-BNL-CCNU, PRD93 (2016) no.1, 014512

curvature of transition line:

$$\kappa_2^t \approx 0.006 - 0.013$$

Cea et al., PRD 93 (2016) no. 1, 014507

Bellwied et al., PLB 751 (2015) 559

Bonati, PRD 92 (2015) no. 5, 054503

Kaczmarek et al., PRD 83 (2011) 014504

Endrodi et al., JHEP 1104 (2011) 001

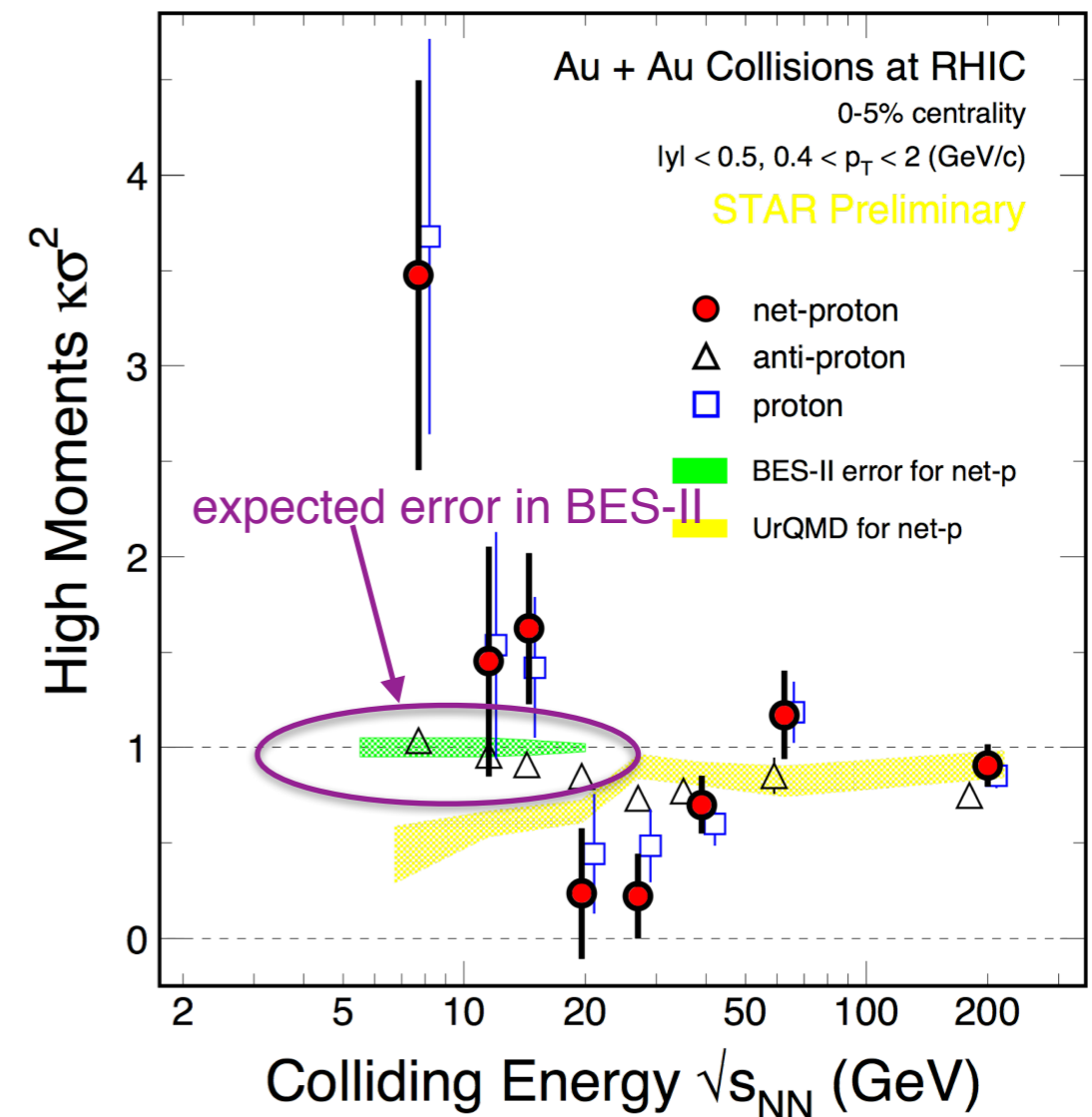
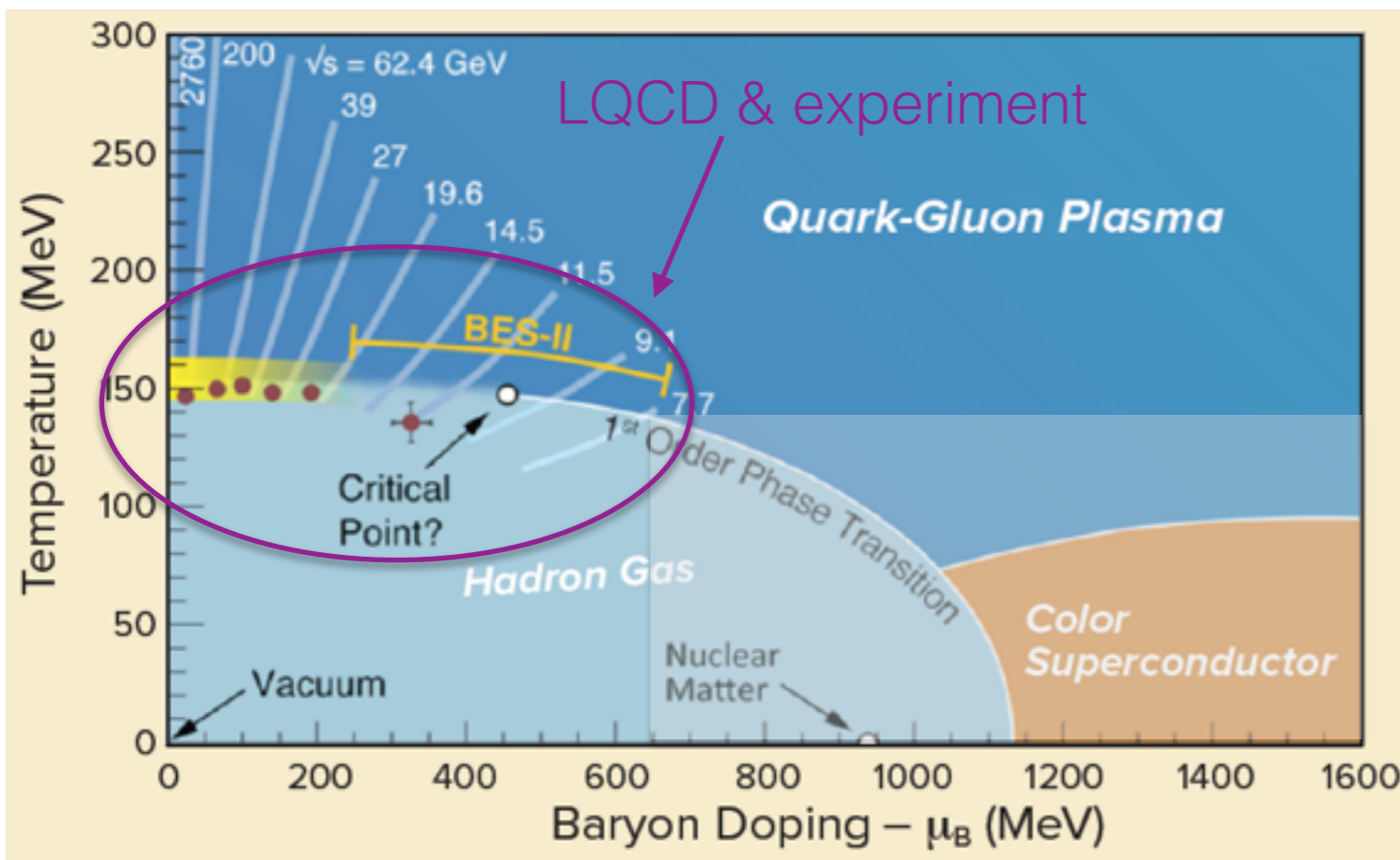


# Outlook: Mapping out the QCD phase diagram

RHIC Beam Energy Scan, Phase II (BES-II)

2019-2020: at least 10 times more statistics for each  $\sqrt{s_{NN}}$

LQCD: higher accuracy for the 6th & 8th or even higher order Taylor expansion coefficients



# hot & dense lattice QCD

Other topics not covered but very important

electrical conductivity & baryon diffusion  
energy loss of heavy quark in hot & dense medium  
thermal dilepton & photon emission from QGP  
shear & bulk viscosities  
fate of heavy quarkonia  
QCD in the external magnetic field

...

See recent reviews:

HTD, F. Karsch, S. Mukherjee, Int. J. Mod. Phys. E 24 (2015) no.10, 1530007  
plenary talks@lattice conference: HTD, arXiv:1702.00151, S. Kim, arXiv:1702.02297  
C. Schmidt & S. Sharma, arXiv:1701.04707  
G. Endrodi, PoS CPOD2014 (2015) 038

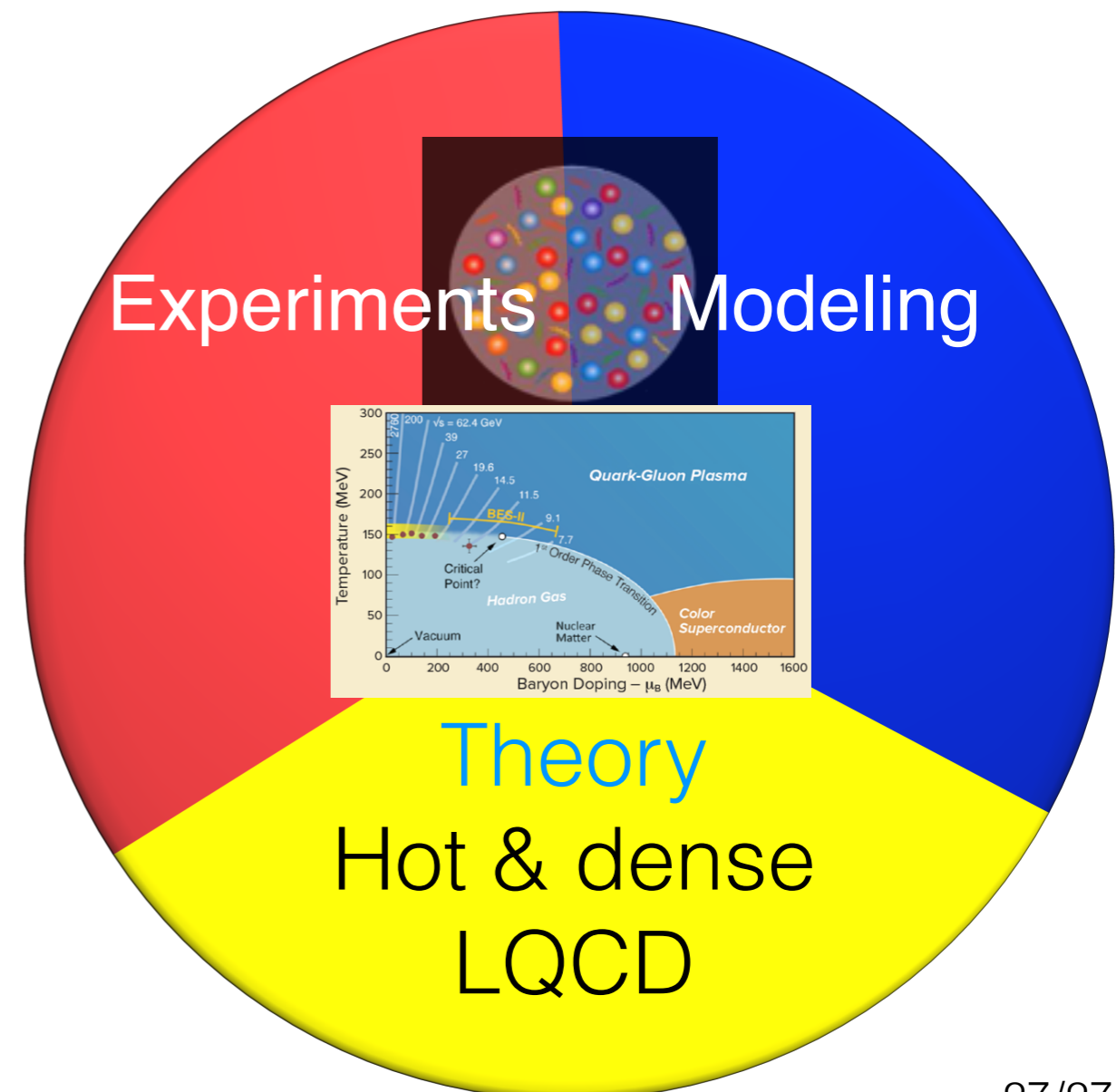
# Summary

In our quest for understanding the properties & phases of strong-interaction matter in extreme conditions

**hot & dense lattice QCD is an essential component**

Interpreting the phenomena observed in HIC experiments needs theory inputs based on lattice QCD

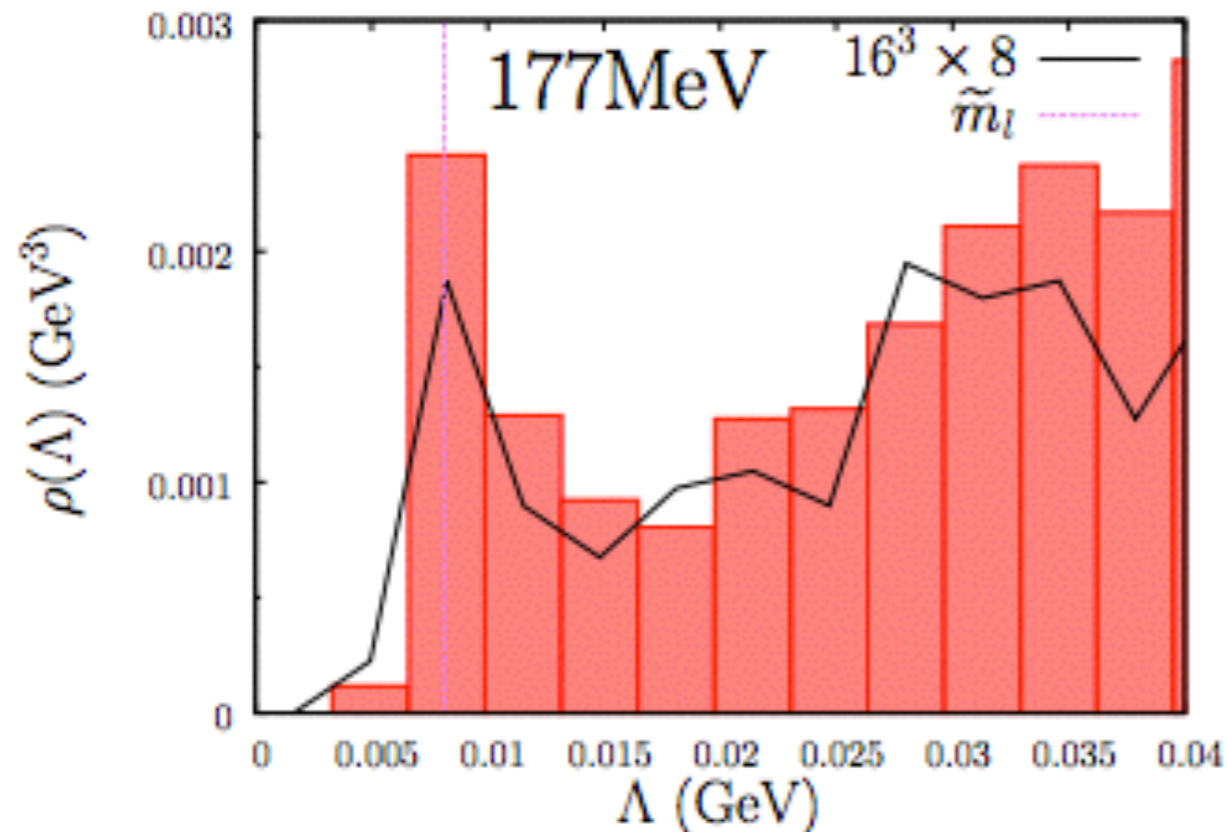
A lot of progress in hot & dense lattice QCD has been made to have close connection with experiments



# Underlying mechanism of $U_A(1)$ breaking

Dirac Eigenvalue spectrum:

black lines:  $16^3$  lattices;  
red histograms:  $32^3$  lattices



Chirality distribution

# of configurations  
with  $N_0$  and  $N_+$   
 $32^3 \times 8, T=177 \text{ MeV}$

$N_+ \setminus N_0$	0	1	2	3	4	5
$N_0 = 1$	40	29	-	-	-	-
$N_0 = 2$	11	20	12	-	-	-
$N_0 = 3$	3	11	6	2	-	-
$N_0 = 4$	0	1	2	1	0	-
$N_0 = 5$	0	2	0	0	0	0

$N_0$ : total # of  
near zero  
modes

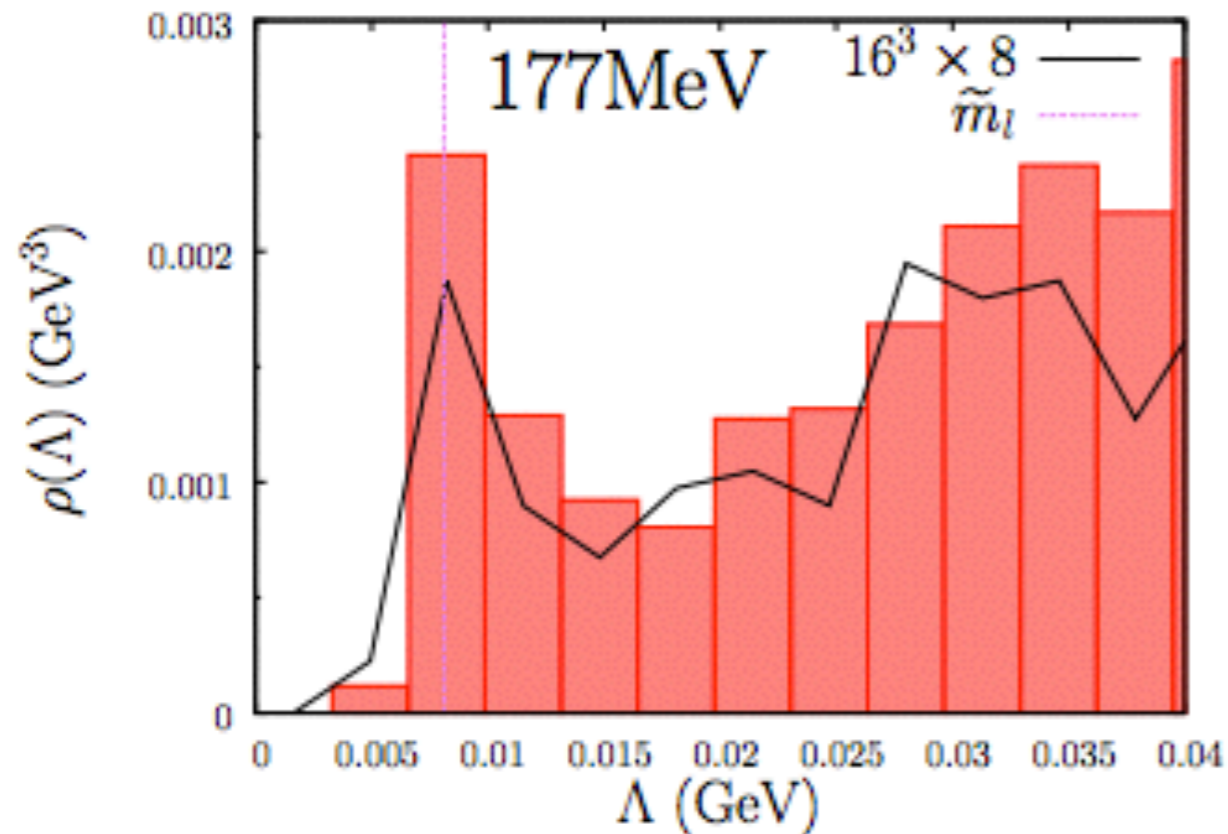
$N_+$ : # of near  
zero modes with  
positive chirality

- Density of near zero modes prefers to be independent of  $V$  rather than to shrink with  $1/\sqrt{32^3/16^3}$
- Chirality distribution shows a binomial distribution more than a bimodal one

# Underlying mechanism of $U_A(1)$ breaking

Dirac Eigenvalue spectrum:

black lines:  $16^3$  lattices;  
red histograms:  $32^3$  lattices



Chirality distribution

# of configurations  
with  $N_0$  and  $N_+$   
 $32^3 \times 8, T=177 \text{ MeV}$

$N_+ \backslash N_0$	0	1	2	3	4	5
$N_0 = 1$	40	29	-	-	-	-
$N_0 = 2$	11	20	12	-	-	-
$N_0 = 3$	3	11	6	2	-	-
$N_0 = 4$	0	1	2	1	0	-
$N_0 = 5$	0	2	0	0	0	0

$N_0$ : total # of  
near zero  
modes

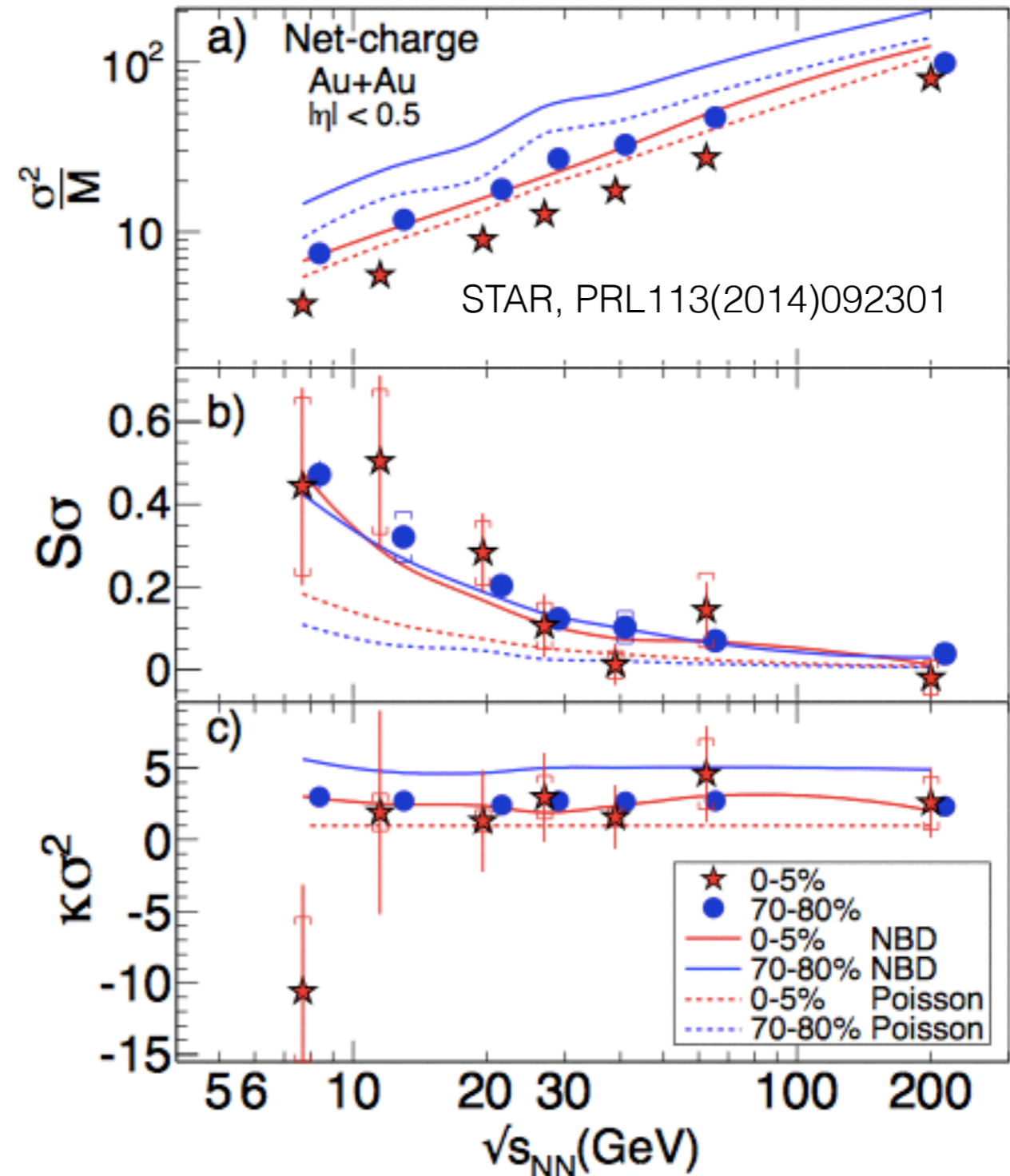
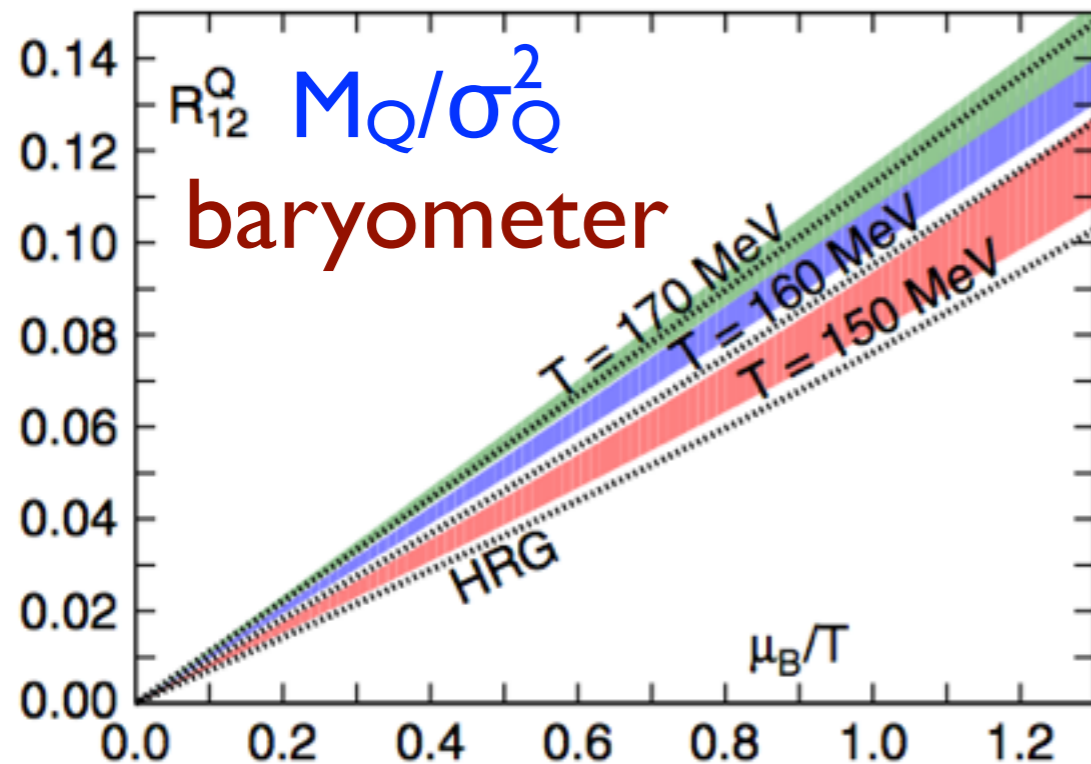
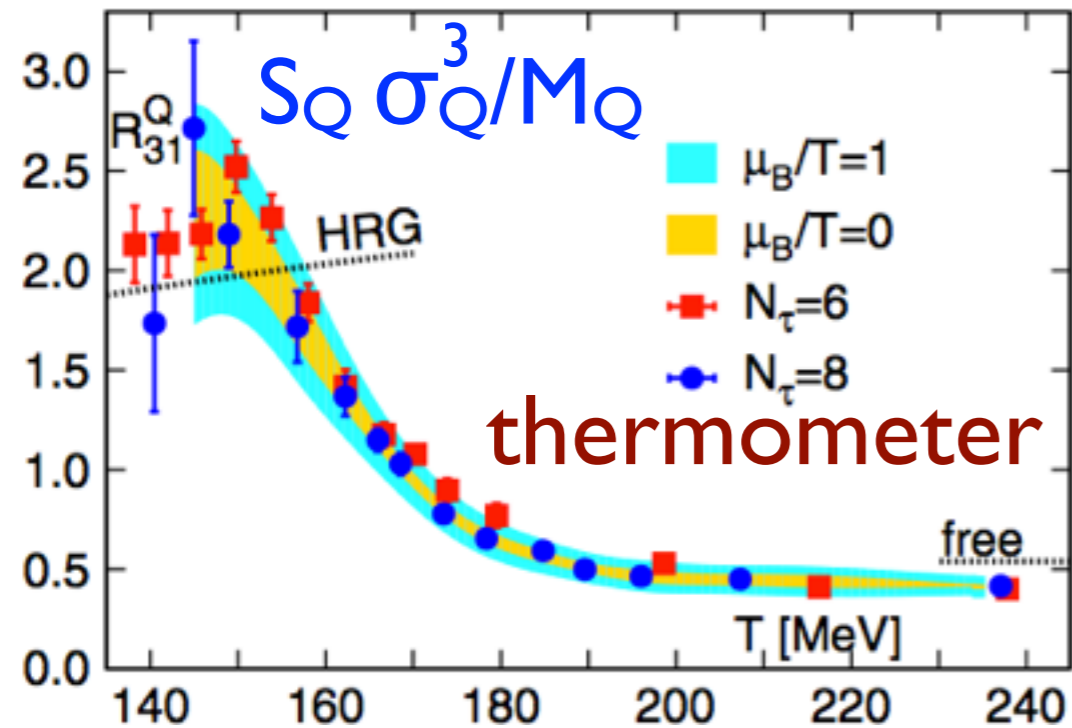
$N_+$ : # of near  
zero modes with  
positive chirality

• Density of near zero modes prefers to be independent of  $V$  rather than **A dilute instanton gas model can describe the non-zero**

• C  **$U_A(1)$  breaking above  $T_c$  !**

bimodal one

# freeze out $T$ and $\mu_B$ from net electrical $Q$ fluctuations as thermo- & baryo- meters



# Beam Energy Scan at RHIC

$\sqrt{s_{NN}}$ (GeV)	Events ( $10^6$ )	BES II / BES I	Weeks	$\mu_B$ (MeV)	$T_{CH}$ (MeV)
200	350	2010		25	166
62.4	67	2010		73	165
39	39	2010		112	164
27	70	2011		156	162
19.6	<b>400</b> / 36	<b>2019-20</b> / 2011	<b>3</b>	206	160
14.5	<b>300</b> / 20	<b>2019-20</b> / 2014	<b>2.5</b>	264	156
11.5	<b>230</b> / 12	<b>2019-20</b> / 2010	<b>5</b>	315	152
9.2	<b>160</b> / 0.3	<b>2019-20</b> / 2008	<b>9.5</b>	355	140
7.7	<b>100</b> / 4	<b>2019-20</b> / 2010	<b>14</b>	420	140

Courtesy of N. Xu